

# PYFLOW v2.5 User's Manual

**A computer code for the calculation of the impact parameters of Dilute  
Pyroclastic Density Currents**

Dr. Dioguardi Fabio, Ph.D.  
06/05/2024

## **License**

PYFLOW 2.5 code

Copyright (C) 2024 Fabio Dioguardi, Pierfrancesco Dellino

Dioguardi F, Mele D (2020) PYFLOW\_2.0: A computer program for calculating flow properties and impact parameters of past dilute pyroclastic density currents based on field data. Bull Volcanol 80, 28 (2018). <https://doi.org/10.1007/s00445-017-1191-z>.

This program is free software: you can redistribute it and/or modify it under the terms of the GNU General Public License as published by the Free Software Foundation, either version 3 of the License, or (at your option) any later version.

This program is distributed in the hope that it will be useful, but WITHOUT ANY WARRANTY; without even the implied warranty of MERCHANTABILITY or FITNESS FOR A PARTICULAR PURPOSE. See the GNU General Public License for more details.

You should have received a copy of the GNU General Public License along with this program. If not, see <http://www.gnu.org/licenses/>.

## **Note for users**

If you wish to contribute to the development of PYFLOW or to reports bugs or other problems with the software, please write an email to [fabio.dioguardi@uniba.it](mailto:fabio.dioguardi@uniba.it)

## Table of Contents

|  |                  |
|--|------------------|
| <b>1. Introduction .....</b>   | <b>3</b>         |
| <hr/>  |                  |
| <b>2. Model .....</b>  | <b>3</b>         |
| <b>2.1. Turbulent Boundary Layer Shear Flows (TBLSF) as an approximation of DPDCs.....</b> | <b>3</b>         |
| <b>2.2. Shield and suspension-sedimentation criterions.....</b>                            | <b>6</b>         |
| <b>2.3. Particle analysis for providing input data.....</b>                                | <b>8</b>         |
| <b><u>2.3.1. Shape dependent drag laws .....</u></b>                                       | <b><u>9</u></b>  |
| <b><u>2.3.2. Particle density.....</u></b>   | <b><u>13</u></b> |
| <b><u>2.3.3. Grainsize distribution analysis.....</u></b>                                  | <b><u>14</u></b> |
| <b>2.4. Two-layers model .....</b>   | <b>15</b>        |
| <b>2.5. Two-components model .....</b>   | <b>18</b>        |
| <b>2.6. Flow stratification model .....</b>  | <b>19</b>        |
| <b><u>2.6.1. Three-equations method .....</u></b>  | <b><u>20</u></b> |
| <b><u>2.6.2. Two-equations method .....</u></b>  | <b><u>21</u></b> |
| <b>2.7 Deposition model .....</b>  | <b>23</b>        |
| <b>2.8. Probability functions of the impact parameters .....</b>                           | <b>26</b>        |
| <hr/>  |                  |
| <b>3. Solution algorithm .....</b>   | <b>27</b>        |
| <hr/>  |                  |
| <b>4. Program setup and execution.....</b>   | <b>30</b>        |
| <b>4.1. Installation .....</b>   | <b>30</b>        |
| <b><u>4.1.1. Linux .....</u></b>   | <b><u>30</u></b> |
| <b><u>4.1.2. Windows and Mac OS .....</u></b>  | <b><u>30</u></b> |
| <b>4.2. Execution .....</b>  | <b>31</b>        |
| <b><u>4.2.1. The input file .....</u></b>  | <b><u>31</u></b> |
| <b><u>4.2.2. The log file .....</u></b>  | <b><u>33</u></b> |
| <b><u>4.2.3. Output files.....</u></b>   | <b><u>34</u></b> |

|                                 |           |
|---------------------------------|-----------|
| <b>5. Test cases .....</b>      | <b>44</b> |
| <b>5.1. Pollena VS2-3.....</b>  | <b>44</b> |
| <b>5.2. Pollena VS26-1.....</b> | <b>49</b> |
| <br>                            |           |
| <b>Reference list .....</b>     | <b>55</b> |
| <br>                            |           |
| <b>Symbol notation .....</b>    | <b>58</b> |

---

## 1. Introduction

---

PYFLOW is a FORTRAN code for the calculation of the flow field variables of dilute pyroclastic density currents (hereafter DPDCs) starting from the deposits characteristics. The code, written in Fortran 90, solves an improved version of the model of Dellino et al. (2008): it calculates the vertical profiles of particle volumetric concentration, flow density, velocity, dynamic pressure, and builds probability functions for each one of these variables. The probability function tool allows to perform a probabilistic analysis of the results and, subsequently, to calculate the parameter of interest at a desired (exceedance) probability. Thanks to these new features, PYFLOW can be used for the assessment of the hazard related to DPDCs, provided that an extensive field study and precise laboratory analyses of the deposits' samples are carried out. In this new version, the code allows the calculation of deposition rates and times from the pyroclastic density current, starting from the flow properties either calculated by the code itself or provided by the user as input. It is in fact possible to run the deposition rate routine as standalone.

Other new features have been added, e.g. an enhanced input data method and the possibility to select among different shape dependent drag laws. The new input data method is based on assignment commands written in an `input.dat` file, which must be included in the same folder as the executable (`pyflow_2.5.exe`).

The program comes as a collection of Fortran files and a script for compiling it and building the executable. The script can be easily modified to use different Fortran compilers under different operating systems.

## 2. Model

---

In this section, the physical models are described. The user should also refer to Dellino et al. (2005, 2008, 2010, 2019a, 2019b), Dioguardi and Dellino (2014), Mele et al. (2011) for further details.

### 2.1. Turbulent Boundary Layer Shear Flows (TBLSF) as an approximation of DPDCs

---

A TBLSF forms when a fluid moves over a solid surface (Furbish, 1997; Schlichting and Gersten, 2000). The analogy between TBLSFs and geophysical surface flows has been proposed for many decades, in particular for the sediment mechanics of particle-laden turbulent flows (Middleton and Southard, 1984). The TBLSF approximation has been already used to calculate average velocity and density of DPDCs of some explosive eruptions at Vulcano, Aeolian Islands (Dellino and La Volpe, 2000, Palizzi eruption) and Campi Flegrei (Dellino et al., 2004, Astroni and Agnano-Monte Spina eruptions). A complete sedimentological model was presented in Dellino et al. (2008) and experimentally validated in Dellino et al. (2010).

In a DPDC, pyroclastic particles are held in suspension by the effect of gas turbulence, as the fluctuating part of velocity directed upward contrasts with the downward particles' settling velocity (Dellino et al., 2008). Indeed, as it follows from Prandtl's assumption (Furbish, 1997; Schlichting and Gersten, 2000) the shear stress at the base of the current is  $\tau_0 = \rho_f u_*^2 = -\rho_f \bar{u}' \bar{w}'$ , where  $\rho_f$  is

the flow density,  $u_*$  is the shear velocity and  $\overline{u'w'}$  is the covariance of the fluctuating velocities in the stream ( $x$ ) and upward ( $z$ ) directions.

A peculiar characteristic of DPDCs is the particle concentration stratification caused by the combined action of gravity and the diffusive effect of the gas turbulence over the particles transported in turbulent suspension. The concentration profile can be calculated by the Rouse equation (Rouse, 1939):

$$C(z) = C_0 \left( \frac{z_0}{z_{tot} - z_0} \frac{z_{tot} - z}{z} \right)^{P_n} \quad (1)$$

where  $C$  is the particle volumetric concentration,  $C_0$  is the particle concentration at the reference level  $z_0$ ,  $z_{tot}$  is the total flow thickness (fig. 1a).  $z_0$  is the base level at which the particles are being settled from suspension, i.e. where  $C(z)$  approaches the maximum packing limit typical of the very thin bedload at the base of a sediment current (that can be assumed to be equal to 0.75, as in Dellino et al. (2008)).  $P_n$  is the Rouse number, a dimensionless quantity defined as:

$$P_n = \frac{w}{ku_*} \quad (2)$$

where  $w$  is the particle settling velocity and  $k$  is Von Karman's constant (equal to 0.4). As it can be easily inferred,  $P_n$  describes the tendency of particles to be transported by a turbulent flow. When  $P_n > 2.5$  a particle is at settling conditions, whereas when  $P_n < 2.5$  it can be held in suspension (Middleton and Southard, 1984). Actually in a DPDC the solid phase is represented by a population of particles, each one characterized by different size, density, drag, i.e. different settling velocity  $w$ . For this reason,  $P_n$  represents an average value of the population.

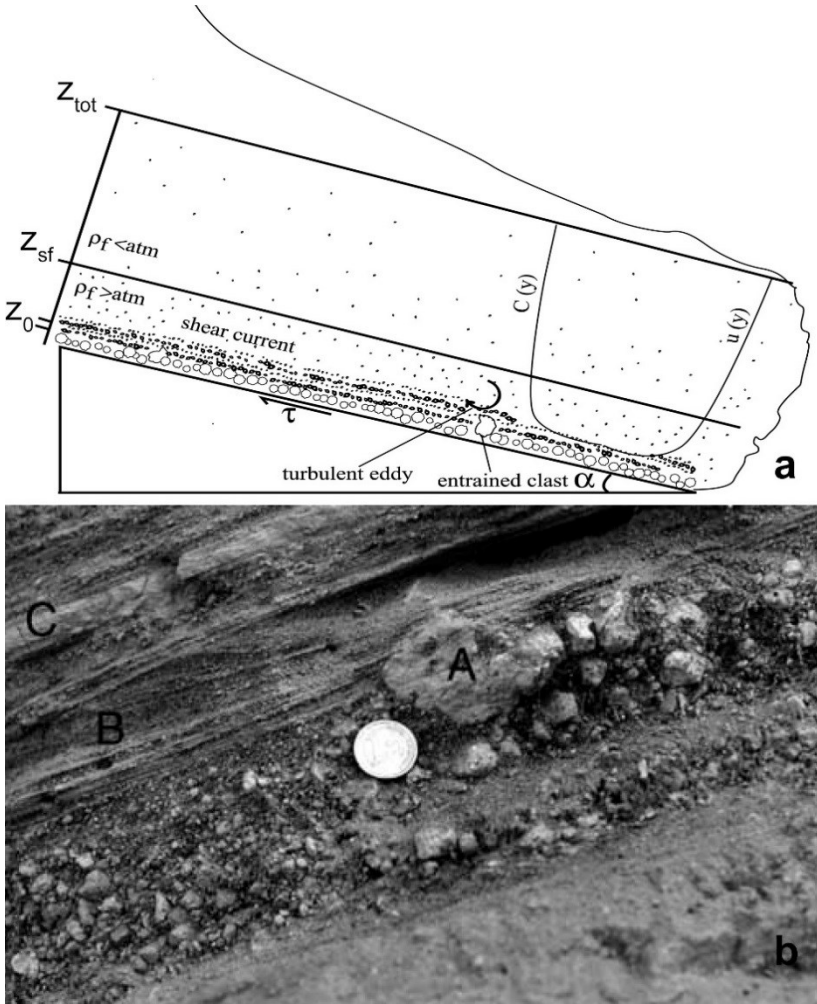


**Figure 1.** **a:** scheme of a DPDC deposit on an inclined slope. The reference level  $z_0$ , the shear flow thickness  $z_{sf}$  and the total flow thickness  $z_{tot}$  are shown, together with the concentration profile  $C(z)$  and average velocity profile  $u(z)$ . **b:** picture of a complete DPDC deposit, with the layer of coarse lapilli and bombs (A), the laminated layer (B) and the massive thin ash layer (C).

The particle concentration profile controls the flow density profile:

$$\rho_f(z) = (1 - C(z))\rho_g + C(z)\rho_s \quad (3)$$

where  $\rho_g$  and  $\rho_s$  are the gas and solid particle density, respectively. As the hot gas is lighter than the atmosphere, and since the current is density stratified, a DPDC can be divided into a basal portion denser than atmosphere (that induces a shear stress on the ground) and an upper portion that is less dense than the atmosphere (fig. 1a). The basal portion is the shear current, which is the part of major interest for the calculation of the DPDCs impact parameters and hazard assessment.

Furthermore, this shear current can be described according to the TBLSF theory (Dellino et al. 2008) and is characterized by the “law of the wall”, which defines the time-averaged velocity profile of the current:

$$\frac{\bar{u}(z)}{u_*} = \frac{1}{k} \ln \frac{z}{k_s} + 8.5 \quad (4)$$

where  $k_s$  is the roughness parameter of the substrate.

In the dense part of the DPDC (i.e. the shear flow), particles settle down from suspension and form the bed load, which represents a minor thickness (less than 1%) compared to the total flow height. The combination of the stress exerted from the overlying shear flow on the bed load, and the continuous sedimentation of particles from suspension, determines a progressive aggradation of sediment to form thin traction laminae (Branney and Kokelaar, 1992; Sulpizio and Dellino, 2008) that sum up and lead to the formation of wavy beds, which are the distinguishing features of DPDCs deposits (Dellino et al., 2008). The complete facies architecture characterizing the stratigraphic sequence of a DPDC deposit is composed of three layers (fig. 1b): (A) a bed of coarse lapilli and bombs representing particle entrained at the base of the current (this layer can be lacking, especially far away from the volcanic vent); (B) a finely laminated layer originated by the lamina by lamina aggradation process described above; (C) a thin massive fine-ash layer representing the fine ash deposited during the waning stage of the flow (Dellino et al., 2004, 2008).

If such a sequence is observed in the field and the beds composing it are described in detail and sampled for successive laboratory investigations, it is possible to use PYFLOW to invert deposit data and define the fluid dynamic characteristics of the parent current. It is to note that the values calculated by PYFLOW represent the current characteristics at the particular location where deposits have been recognized in the field. In the case that multiple outcrops of deposits of a DPDC are found, by applying PYFLOW to each of them, it would be possible to define the variation of pyroclastic density current behaviour over the dispersal area. It is to recall that the model is based on the TBLSF approximation of DPDCs, thus it is expected to give reliable results only in the case of dilute currents. In fact, Dellino et al. (2008) carried out a stress test in which it was shown that, upon applying the model to a thick massive deposit related to a highly concentrated flow of the Pollena eruption at Vesuvius, the t-Student test (which will be presented below) fails, thus indicating that the model is not applicable if samples come from deposits that are not formed from dilute density currents. The t-Student test is therefore a check of both the applicability of the PYFLOW model and of the reliability of results.

## 2.2. Shield and suspension-sedimentation criterions

---

In a DPDC, there are particles that are never transported in suspension but can be moved over the substrate by the current shear stress (e.g. particles with  $P_n$  much higher than 2.5 or particles already lying on the ground before the DPDC passage). This phenomenon can be described by the Shield or entrainment criterion (Miller et al., 1977), which compares the DPDC shear stress to the buoyancy force of the coarse particle in the flow:

$$\theta = \frac{\rho_f u_*^2}{(\rho_{s1} - \rho_f)gd_1} \quad (5)$$

where  $g$  is gravity acceleration,  $\rho_{s1}$  and  $d_1$  the density and diameter of the entrained particle, respectively;  $\theta$  is a parameter depending on the particle shear Reynolds number  $Re^*$  ( $Re^* = \rho_f u_* d_1 / \eta$  where  $\eta$  is the fluid viscosity), which is equal to 0.015 for a  $Re^*$  number larger than 1000

(Miller et al., 1977). This is a condition that can be reasonably considered to be common in most DPDCs since, if one considers a clast of 2 cm diameter (generally clasts moved at the base of pyroclastic density currents are even coarser), 1500 kg m<sup>-3</sup> density and a shear current with a shear velocity of 1 m s<sup>-1</sup> and a kinematic viscosity of 1.6\*10<sup>-5</sup> Pa s (reasonable values even for quite small DPDCs with a fluid phase represented by gases at 300 °C),  $Re^*$  is about 1.8\*10<sup>6</sup>, hence much higher than 1000.

On the other hand, at the limit of transportation by turbulent suspension when  $P_n = 2.5$ , from eq. (2), since  $k = 0.4$ , it follows that:

$$w = u_* \quad (6)$$

This is the suspension-sedimentation criterion (Middleton and Southard, 1984), which means that particles stay suspended until their settling velocity is less than flow shear velocity. In other terms, particles in the deposit that are settled from suspension (the laminae-forming bed load) give an indication of the current shear velocity, once their terminal velocity is defined. Particle settling velocity  $w$  can be calculated by the so-called Newton impact law:

$$w = \sqrt{\frac{4gd(\rho_s - \rho_f)}{3C_d\rho_f}} \quad (7)$$

where  $d$  is the particle equivalent diameter (i.e. the diameter of the sphere having the same volume of the settling particle),  $C_d$  is the drag coefficient. Upon combining (6) and (7), it follows that:

$$u_*^2 = \frac{4gd(\rho_s - \rho_f)}{3C_d\rho_f} \quad (8)$$

The shear velocity is actually the shear stress at the base of the current normalized by the flow density:

$$\tau = \rho_f u_*^2 \quad (9)$$

When the stratigraphic sequence described in the previous section is recognized in the field (fig. 1b: 1) the coarse layer of lapilli and bombs moved by shear at the base of the current; 2) the laminated layer of ash formed by particles settled from turbulent suspension) it is possible to apply both the Shield (twolayers model) and the suspension-sedimentation (twocomponents model) criteria for calculating the flow parameters. However, the layer of entrained coarse lapilli or bombs, which is typical of proximal locations around the eruptive vent, is often missing in distal outcrops, thus preventing to use the Shield criterion far away from the volcanic vent. In that case, an alternative method based on the hydraulic equivalence of particles can be used. The system of equation to be applied in the two cases will be discussed in the sections 2.4 and 2.5.

## 2.3. Particle analysis for providing input data

---

(Hereafter each time a new variable needed in input is presented, the related keyword in the `input.dat` is written in brackets and capital letters. See Section 4.2.1)

In order to use eqs. (5) to (9) and solve for the flow shear velocity and density, it is necessary to provide in input, besides layer properties (layer thickness  $z_{lam}$  (ZLAM), substrate roughness  $k_s$  (KS), sublayer thickness  $z_0$  (ZLAMS)), physical properties of the particles representing the laminated layer and possibly the basal coarse layer (Fig. 1b). In particular, for the aforementioned two models the following data are strictly needed:

- `twolayers` model: density  $\rho_{s1}$  (DENS\_ENT) and representative dimension  $d_1$  (DM\_ENT) of the selected particle in the coarse layer; density  $\rho_s$  (RHOS(i=1,j=0), where i and j are the indexes identifying the component and the grainsize classes, respectively; when `twolayers` model is used, data of the component i=1 are only used; j=0 is the grainsize class representative of the component, usually the median), the representative dimension  $d$  (either PHI50(i=1) or D50MM(1), respectively in phi units and mm) and shape of the particle deposited in the laminated layer (depending on the chosen drag law CDLAW(i), see Table 1), possibly of a selected component (e.g. juvenile glassy particles or crystals, depending on the relative abundance).
- `twocomponents` model: density  $\rho_s$ , representative dimension  $d$  and shape of the particle deposited in the laminated layer of two selected components (RHOS(1,0), RHOS(2,0), PHI50(1) or D50MM(1), PHI50(2) or D50MM(2), CDLAW(1), CDLAW(2)).

For the entrained clast at the base of the current,  $d_1$  can be measured by means of a calliper by taking the geometric mean between the three axes. Alternatively,  $d_1$  can be calculated as the diameter of the equivalent sphere  $d_{sph}$  by measuring the weight  $m$  and the density  $\rho_{s1}$  of the clast.

$$d_1 = d_{sph} = \sqrt[3]{\frac{6m}{\pi\rho_{s1}}} \quad (10)$$

Density  $\rho_{s1}$  can be measured with a standard pycnometer. For the particles in the laminated layer,  $d$  could be, for example, the equivalent diameter of the median size of the grainsize distribution of the selected layer component. Furthermore, shape descriptors and density  $\rho_s$  of particles of dimension  $d$  (i.e. measured from samples selected from the median grainsize class) coming from the laminated layer are needed in order to compute the drag coefficient  $C_d$ . The type of the needed shape descriptor depends on the selected shape-dependent drag law, as it will be explained in the following section.

The representative particle size from the laminated layer of a selected component  $d$  is the median grainsize measured in mm. In input, the user must provide this value (or the value in phi units,  $Md_\phi$ ) together with the sorting  $\sigma_\phi$  of the grainsize distribution. Alternatively, the user can let the program calculate these values for either component 1 or 2 or both by running the grainsize analysis utility and providing the complete grainsize distributions in input, either as mass (gr) or weight fraction (%) over the whole sample) (see Section 2.3.3).

Since pyroclastic particles are not well approximated by spheres (Dellino et al., 2005),  $Md_\phi$  is adjusted by the average value of the diameter (in phi units) of the equivalent sphere of particles

selected from the grainsize class where the median lies ( $d_{avg eq sph}$ ), if this is available. In this case, the normalization proceeds in this way:  $d_{avg eq sph}$  is first standardized by means of the median and sorting of the grainsize distribution:

$$Z_{d_{avg eq sph}} = \frac{d_{avg eq sph} - Md_\phi}{\sigma_\phi} \quad (11)$$

By using the normalized standard distribution, the cumulative probability associated with  $Z_{d_{avg eq sph}}$  is calculated:

$$P(Z_{d_{avg eq sph}}) = \frac{1}{2} \left( 1 + erf \left( \frac{Z_{d_{avg eq sph}}}{2} \right) \right) \quad (12)$$

Since the cumulative probability associated with  $Z_{Md\phi_{norm}}$  which is the standard variable of the median grainsize  $Md_\phi$  normalized by this procedure, is 0.5 by definition, from proportionality one can write:

$$Z_{Md\phi_{norm}} = \frac{0.5 * Z_{d_{avg eq sph}}}{P(Z_{d_{avg eq sph}})} \quad (13)$$

From the definition of a standardized variable,  $Md\phi_{norm}$  is readily obtained:

$$Md\phi_{norm} = Md\phi + Z_{Md\phi_{norm}} \sigma_\phi \quad (14)$$

$Md\phi_{norm}$  is finally converted in mm to get  $d$ .

### **2.3.1. Shape dependent drag laws**

---

In the new version, it is possible to choose among nine shape-dependent drag formulas. Volcanic particles cannot be approximated as spheres, especially in the fluid dynamic regimes typical of DPDCs. It is well known, in fact, that the influence of particle shape increases as the particle Reynolds number  $Re$  increases (Ganser, 1993; Dioguardi and Mele, 2015; Bagheri and Bonadonna, 2016; Dioguardi et al., 2017). Therefore, in order to obtain realistic estimates of DPDCs impact parameters, it is essential to use shape dependent drag formulas. These drag formulas are generally a function of  $Re$  and one or more particle shape descriptors. The following table summarizes the possible choices, the needed shape descriptors and the appropriate reference. It is to note that the code allow to calculate the drag assuming spherical particles with the command “SPHERE”; in this case the drag is calculated by using the formula of Clift and Gauvin (1971). The available drag laws are listed in Table 1.

**Table 1.** List of shape-dependent drag laws available in PYFLOW v2.5, together with the commands

| Drag law                     |                        | Shape                                     |   |
|------------------------------|------------------------|---|---|
| Reference                    | Command<br>(CDLAW=...) | Shape descriptor                          | Command                                     |
| Clift and Gauvin (1971)      | 'SPHERE'               | -   | -   |
| Haider and Levenspiel (1989) | 'HAIDLEV'              | Sphericity $\varphi$                      | SPHERICITY(i,j)                             |
| Swamee and Ojha (1991)       | 'SWAMOJ'               | Corey Shape Factor $\beta$                | COREY(i,j)                                  |
| Ganser (1993)                | 'GANSER'               | Isometric particle                        | Sphericity $\varphi$                        |
|                              |                        | Non isometric particle                    | Sphericity $\varphi$                        |
|                              |                        |   | Volume equivalent sphere diameter $d_{sph}$ |
|                              |                        |   | Circle equivalent sphere diameter $d_{pr}$  |
| Chien (1994)                 | 'CHIEN'                | Sphericity $\varphi$                      | SPHERICITY(i,j)                             |
| Tran-Cong et al. (2004)      | 'TRANCONG'             | Circularity $c$                           | CIRCULARITY(i,j)                            |
|                              |                        | Flatness ratio $\gamma$                   | FLATRATIO(i,j)                              |
| Dellino et al. (2005)        | 'DELLINO'              | Shape Factor $\Psi$                       | SHAPEFACT(i,j)                              |
| Hölzer and Sommerfeld (2008) | 'HOLZOMM'              | Sphericity $\varphi$                      | SPHERICITY(i,j)                             |
|                              |                        | Longwise sphericity $\varphi_{\parallel}$ | LONGSPHER(i,j)                              |
|                              |                        | Crosswise sphericity $\varphi_{\perp}$    | CROSSSPHER(i,j)                             |
| Dioguardi and Mele (2015)    | 'DIOGMELE'             | Shape Factor $\Psi$                       | SHAPEFACT(i,j)                              |
| Dioguardi et al. (2017)      | 'DIOG2017'             | 3D Fractal Dimension $D_{3D}$             | FRACTDIM(i,j)                               |
|                              |                        | 3D Sphericity $\varphi_{3D}$              | SPHERICITY(i,j)                             |
| Dioguardi et al. (2018)      | 'DIOG2018'             | Shape Factor $\Psi$                       | SHAPEFACT(i,j)                              |

### Clift and Gauvin (1971)

$$C_d = C_{d,sphere} = \frac{24}{Re} [1 + 0.15Re^{0.687}] + \frac{0.42}{1 + \frac{42500}{Re^{1.16}}} \quad (15)$$

Haider and Levenspiel (1989)

$$C_d = \frac{24}{Re} (1 + A Re^B) + \frac{C}{1 + \frac{D}{Re}} \quad (16)$$

$$A = \exp(2.329 - 6.458\varphi + 2.449\varphi^2) \quad (16a)$$

$$B = 0.0964 + 0.5565\varphi \quad (16b)$$

$$C = \exp(4.905 - 13.894\varphi + 18.422\varphi^2 - 10.26\varphi^3) \quad (16c)$$

$$D = \exp(1.468 - 12.258\varphi + 20.732\varphi^2 - 15.886\varphi^3) \quad (16d)$$

Swamee and Ojha (1991)

$$C_d = \left\{ \frac{48.5}{(1 + 4.5\beta^{0.35})^{0.8} Re^{0.64}} + \left[ \left( \frac{Re}{Re + 100 + 100\beta} \right)^{0.32} \frac{1}{\beta^{18} + 1.05\beta^{0.8}} \right] \right\} \quad (17)$$

Ganser (1993)

$$C_d = \frac{24}{Re K_1 K_2} [1 + 0.1118(Re K_1 K_2)^{0.6567}] + \frac{0.4305}{1 + \frac{3305}{Re K_1 K_2}} \quad (18)$$

where  $K_1$  and  $K_2$  are shape factors defined in the following way:

|                      | $K_1$   | $K_2$                                 |
|----------------------|---|---------------------------------------|
| Isometric shapes     | $\left[ \frac{1}{3} + \left( \frac{2}{3} \right) \varphi^{-0.5} \right]^{-0.1}$             | $10^{1.8148(-\log \varphi)^{0.5743}}$ |
| Non-isometric shapes | $\left[ \frac{d_{sph}}{3d_{pr}} + \left( \frac{2}{3} \right) \varphi^{-0.5} \right]^{-0.1}$ | $10^{1.8148(-\log \varphi)^{0.5743}}$ |

Chien (1994)

$$C_d = \frac{30}{Re} + 67.289 e^{-5.03\varphi} \quad (19)$$

Tran-Cong et al. (2004)

$$C_d = \frac{24}{Re} \gamma \left[ 1 + \frac{0.15}{\sqrt{c}} (\gamma Re)^{0.687} \right] + \frac{0.42\gamma^2}{\sqrt{c} [1 + 4.25 \times 10^4 (\gamma Re)^{-1.16}]} \quad (20)$$

Dellino et al. (2005)

$$C_d = \frac{0.9297}{\Psi^{1.6} Re^{0.0799}} \quad (21)$$

It is to note that the authors developed a formula for calculating the terminal velocity of irregular particles that avoids the explicit and circular dependency of  $C_d$  on  $Re$ , which forces the implementation of an iterative calculation. This is as follows:

$$w = \frac{1.2065\eta \left[ \frac{d^3 g (\rho_s - \rho_f) \rho_f \Psi^{1.6}}{\eta^2} \right]^{0.5206}}{d\rho_f} \quad (21a)$$

### Hölzer and Sommerfeld (2008)

$$C_d = \frac{8}{Re} \frac{1}{\sqrt{\varphi_{\parallel}}} + \frac{16}{Re} \frac{1}{\sqrt{\varphi}} + \frac{3}{\sqrt{Re}} \frac{1}{\varphi^{0.75}} + 0.4210^{0.4(-\log \varphi)^{0.2}} \frac{1}{\varphi_{\perp}} \quad (22)$$

### Dioguardi and Mele (2015)

$$C_d = \frac{C_{d,sphere}}{Re^2 \Psi^{Re^{-0.23}}} \left( \frac{Re}{1.1883} \right)^{\frac{1}{0.4826}}, Re < 50 \quad (23a)$$

$$C_d = \frac{C_{d,sphere}}{Re^2 \Psi^{Re^{0.05}}} \left( \frac{Re}{1.1883} \right)^{\frac{1}{0.4826}}, Re > 50 \quad (23b)$$

where  $C_{d,sphere}$  is the drag coefficient of the sphere at the same Reynolds number  $Re$ . In this model the law of Clift and Gauvin (1971) is considered as a good approximation of  $C_{d,sphere}$  (eq. 15).

### Dioguardi et al. (2017)

If the 3D fractal dimension  $D_{3D}$  is used as shape descriptor:

$$C_d = \frac{4}{3} \frac{0.3492 C_{d,sphere} (Re^{1.62} D_{3D}^{Re^{-0.13}})^{1.3358}}{Re^2} \quad (24a)$$

otherwise if the shape descriptor is the 3D sphericity  $\varphi_{3D}$ :

$$C_d = \frac{4}{3} \frac{0.559 C_{d,sphere} (Re^{4.18} \varphi_{3D}^{-Re^{-0.2}})^{0.5134}}{Re^2} \quad (24b)$$

Note that 3D sphericity can be given in input with the same command as for the approximate sphericity  $\varphi$ , SPHERICITY(i,j).

## ***Dioguardi et al. (2018)***

Like Dellino et al. (2005) and Dioguardi and Mele (2015), this is a function of the particle shape factor  $\psi$ :

$$C_d = \frac{24}{Re} \left( \frac{1 - \psi}{Re} + 1 \right)^{0.25} + \frac{24}{Re} (0.1806 Re^{0.6459}) \psi^{-Re^{0.08}} + \frac{0.4251}{1 + \frac{6880.95}{Re} \psi^{5.05}} \quad (25)$$

### **2.3.2. Particle density**

PYFLOW offers greater flexibility when providing particle density in the laminated layer. This was necessary when implementing the new deposition model (Section 2.5). In this model, in fact, the deposition rates of each grainsize class of each component constituting the deposit are calculated and then summed to obtain the total deposition rate. For juvenile vesiculated particles, density can change significantly with size (Houghton and Wilson (1989); Dellino et al. (2005); Beckett et al. (2015)); in turn, density significantly influences deposition rate (eq. 48). Hence, PYFLOW now allows to either specify a constant or a size-dependent density, in the latter case either by indicating the density of each grainsize class or using built-in density-size functions, which were obtained by available data from previous studies. The command RHO\_LAW(i) can be used to inform PYFLOW how to consider particle density for the  $i^{\text{th}}$  component. The following cases are possible:

- 1) RHO\_LAW(i)=’CUSTOM’. In this case, the user needs to indicate the representative density of the component i; this in turn is done by specifying RHOS(i,0)=”a number” (e.g. RHOS(2,0)=2500). Note that the index “j=0” refers to the median grainsize class, whose density is needed for the two-layers or two-components model. If the deposition model is activated, an additional information is needed:
  - the custom density is constant (RHO\_CUSTOM(i)=’CONSTANT’): the density of all the grainsize classes are assumed equal to the provided density of the median class
  - the custom density is variable (RHO\_CUSTOM(i)=’VARIABLE’): the user needs to provide in input the density of each single grainsize class with the command “RHOS(i,j)”, where “i” and “j” are integer numbers identifying the component and the grainsize class, respectively (e.g. RHOS(1,2)=1700, RHOS(1,5)=2400, etc.).
- 2) RHO\_LAW(i)=’SIAL\_XX’:  $\rho_s = 2400 \text{ kg m}^{-3}$ , a typical value for sialic crystals.
- 3) RHO\_LAW(i)=’FEM\_XX’:  $\rho_s = 3280 \text{ kg m}^{-3}$ , a typical value for mafic crystals (pyroxenes).
- 4) RHO\_LAW(i)=’LITHIC’:  $\rho_s = 2570 \text{ kg m}^{-3}$ , a typical value for lithic particles.
- 5) Some additional options are available for automatically obtaining a size-dependent density of juvenile vesiculated particles for specific real cases. These are summarized in Table 2. It is to note that the empirical law can let particle density be larger than the dense rock equivalent density of the specific sample when particle size becomes very small, in which case a limiting value is imposed.

**Table 2.** List of available empirical laws for calculating the size-dependent density of juvenile vesiculated particles

| Command   | Equation                                | Limiting value          | Reference             |
|-----------|---|-------------------------|-----------------------|
| 'POLLENA' | $\rho_s = (-0.31 \log d + 1.83) * 1000$ | 2760 kg m <sup>-3</sup> | Dellino et al. (2008) |
| 'AVERNO2' | $\rho_s = (-0.3 \log d + 1.42) * 1000$  | 2600 kg m <sup>-3</sup> | Dellino et al. (2008) |
| 'AMS'     | $\rho_s = (1.06d^{-0.332}) * 1000$      | 2560 kg m <sup>-3</sup> | <i>This work</i>      |
| 'POMPEI'  | $\rho_s = (1.822d^{-0.167}) * 1000$     | 2700 kg m <sup>-3</sup> | <i>This work</i>      |
| 'MERCATO' | $\rho_s = (0.956d^{-0.191}) * 1000$     | 2400 kg m <sup>-3</sup> | L'Abbate (2007)       |
| 'ASTRONI' | $\rho_s = (0.812d^{-0.213}) * 1000$     | 2510 kg m <sup>-3</sup> | Manzaro (2005)        |

### **2.3.3. Grainsize distribution analysis**

PYFLOW offers the possibility to perform grainsize distribution analysis for the two components used in the sedimentological model (Sections 2.4, 2.5) in order to calculate the median  $Md_\phi$  and sorting  $\sigma_\phi$ . This function can be activated by the commands “DISTR1 = .T.” (for component 1) and “DISTR2 = .T.” (for component 2) in the input file. Note that, if the depositional model is also activated (Section 2.5), the program will perform grainsize analysis by default for all the components considered for this model, since the user will be forced to provide grainsize and density distribution data.

For running the grainsize analysis, the program requires the minimum and maximum grainsize (“PHIMIN(i)”, “PHIMAX(i)”) and the grainsize interval (“DPHI(i)”) of the distribution in phi units. Furthermore, the weights of each grainsize class have to be specified with the command “WEIGHT(i,j)”. It is to note that, based on the provided minimum and maximum grainsize and the grainsize interval, PYFLOW calculates the number of grainsize classes  $n_{classes}$  for each component and checks if the weights of all the  $n_{classes}$  classes are listed in the input file. Any missing input will generate an error message with an indication of what command is missing. Additionally, the user can choose if to provide the weights as weight fraction over the entire sample (“INPUT\_WEIGHT=’WT’”) or mass (“INPUT\_WEIGHT=’MASS’”). Finally, a Chi-squared ( $\chi^2$ ) test for checking if the distribution is significantly different from a normal Gaussian distribution can be optionally activated with the command “DOTESTCHI(i)=.T.”, in which case the user needs to supply the program with the significance level of the test  $\alpha_{test}$  (“SIGLEVCHI(i)”). It is recommended to always perform this statistical test, since the central tendency parameters calculated by PYFLOW and that are subsequently used in the flow calculations, i.e. the median and sorting, are calculated with the assumption that the grainsize distribution is not significantly different from a normal Gaussian distribution, a condition that sometimes is not satisfied.

The test proceeds in this way. The grainsize distribution is rearranged to merge all the grainsize classes with a weight fraction <5% (calculated over the weight of the single component, not of the entire sample). The 5% limit is a default value that can be changed by the user with the command

“SENSCHI(i)”. The so rearranged grainsize distribution represents a vector of observed values  $O_j$ . After this step, the grainsize limits in phi units  $d_{\phi,j}$  are standardized by using the median  $Md_\phi$  and sorting  $\sigma_\phi$  of the distribution:

$$Z_{test,j} = \frac{d_{\phi,j} - Md_\phi}{\sigma_\phi} \quad (26)$$

With these standardized grainsizes, the program calculates the corresponding observed frequencies  $E_j$  by integrating the probability density function of the normalized standard distribution:

$$E_j = \frac{1}{2} \left( 1 + \operatorname{erf} \left( \frac{Z_{test,j}}{\sqrt{2}} \right) \right) \quad (27)$$

The  $\chi^2$  variable is then calculated with the following formula:

$$\chi^2_{calc} = \sum_{j=1}^{n_{classes}} \frac{(O_j - E_j)^2}{E_j} \quad (28)$$

and is compared to the theoretical value of the  $\chi^2$  variable at the desired significance level  $\alpha_{test}$  and  $n_{classes}-3$  degrees of freedom, where 3 is the number of constraining variables, in this case the two used central tendency parameters (median and sorting) and the condition that the sum of weight fraction must sum up to 1 (100%). The theoretical values corresponding to the significance level are tabulated but PYFLOW calculates them automatically by solving the following equation:

$$\alpha_{test} = \int_x^\infty \frac{1}{2^{\frac{K}{2}} \Gamma(\frac{K}{2})} x^{\frac{K}{2}-1} e^{-\frac{x}{2}} \quad (29)$$

where  $\Gamma$  is the Gamma function and  $x = \chi^2_{teor}$ . This equation is solved numerically by using the false position method (Press et al., 1996), with the integral evaluated numerically with the trapezoid method following Simpson’s rule (Press et al., 1996). The grainsize distribution is not different from a normal standard distribution at a significance level  $\alpha_{test}$  if  $\chi^2_{calc} < \chi^2_{teor}$ .

## 2.4. Two-layers model

---

When the complete fining upward sequence (fig. 1b) is observed in the deposit, it can be assumed that during the depositional history of the DPDC, at the interface between the basal and laminated layers the coarse particles lying on the substrate (or in the forming deposit) were just moved by the shear stress at the base of the current (Dellino et al., 2008). The overlying laminae are formed by particle settling from turbulent suspension. The interface between the two layers represent the zone of maximum shear stress in the current. The value of shear velocity and density resulting from the

solution of the system of equations 5, 8 and 9 thus represent the characteristics of the shear current at the considered location where the sample has been collected.

It is to remark that the parameters on the right side of eq. 8 refer to a population of particles rather than single particles, and therefore represent average values over the entire population. The average value is the equivalent diameter of the median size  $d$ ; the range of variation is represented by the sorting  $\sigma_\phi$  of the grain-size distribution. Consequently, also the drag coefficient  $C_d$ , which is a function of  $d$  varies accordingly. In order to better evaluate the range of solutions (shear velocity and flow density) of the system of equations 5 and 8, it is convenient to group the parameters having a range of variation ( $d$  and  $C_d$ ) in a ratio  $C_d/d$ . Upon rearranging the equations:

$$\frac{C_d}{d} = \frac{4(\rho_s - \rho_f)}{d_1 \theta 3(\rho_{s1} - \rho_f)} \quad (30)$$

A range of values is calculated as a function of a realistic range of flow density  $\rho_f$ . As stated in Section 1, the shear current is denser than atmosphere; furthermore, the particle volumetric concentration is expected to be limited to a few percent, in order to conform to the dilute current assumption. Thus, a reasonable range of flow density is between 2 and 100 kg m<sup>-3</sup>. The validity of this assumption has been discussed in detail and validated in Dellino et al. (2008).

The values of  $C_d/d$  corresponding to realistic flow density values are named  $C_d/d(2 \text{ kg m}^{-3})$  and  $C_d/d(100 \text{ kg m}^{-3})$ . By isolating  $\rho_f$  in eq. 5 and substituting it into (30), the ratio  $C_d/d$  as a function of the squared shear velocity is obtained:

$$\frac{C_d}{d} = \frac{4g \left( \rho_s - \frac{\theta gd_1 \rho_{s1}}{u_*^2 + \theta gd_1} \right)}{3u_*^2 \left( \frac{\theta gd_1 \rho_{s1}}{u_*^2 + \theta gd_1} \right)} \quad (31)$$

Substituting the values of  $C_d/d(2 \text{ kg m}^{-3})$  and  $C_d/d(100 \text{ kg m}^{-3})$  into (31), the corresponding values of the squared shear velocity  $u_*^2 (2 \text{ kg m}^{-3})$  and  $u_*^2 (100 \text{ kg m}^{-3})$  are calculated. By using the theorem of the average value of a function, the average model ratio of  $C_d/d$  is found:

$$\frac{C_d}{d} avg = \frac{1}{u_*^2_{2 \text{ kg/m}^3} - u_*^2_{100 \text{ kg/m}^3}} \int_{u_*^2_{100 \text{ kg/m}^3}}^{u_*^2_{2 \text{ kg/m}^3}} \frac{4g \left( \rho_s - \frac{\theta gd_1 \rho_{s1}}{u_*^2 + \theta gd_1} \right)}{3u_*^2 \left( \frac{\theta gd_1 \rho_{s1}}{u_*^2 + \theta gd_1} \right)} du_*^2 \quad (32)$$

With the same approach the average particle drag coefficient  $C_d$  can be calculated in the 2-100 kg m<sup>-3</sup> flow density range:

$$C_d avg = \frac{1}{100 - 2} \int_2^{100} C_d(Re, Shape) d\rho_f \quad (33)$$

$C_d avg$  can be considered to be a good estimate of the population of particles settling from turbulent suspension if the grain-size distribution approximates a Gaussian curve, which is usually the case of

this kind of samples and can be verified by performing the Chi-Squared test when `grainsize` is invoked (Section 2.3.3). A model value for the particles diameter can be obtained by the following relationship:

$$d_{mod} = \frac{C_d avg}{\frac{C_d}{d} avg} \quad (34)$$

This value can be compared with that measured from the sample  $d$  by means of a statistical Student  $t$ -test, by defining the  $t$  variable as:

$$t = \frac{Md\phi_{norm} - d_{mod}}{\sigma_\phi \sqrt{\frac{1}{n}}} \quad (35)$$

The degrees of freedom  $n$  are equal to  $n_{classes} - 1$ . At this point PYFLOW performs a two-tails test; by default, the significance level of the statistical test is set to 0.05, but the user can set a different value. If the  $t$ -test succeeds,  $d_{mod}$  is an appropriate model of the experimental data, meaning that the initial assumption that  $2 \text{ kg m}^{-3} < \rho_f < 100 \text{ kg m}^{-3}$  is reasonable and the model results are a significant solution of actual deposit data. The  $t$  value at the significant level of 0.05 is known and tabulated but, as PYFLOW allows to change the significance level, the code searches for the  $t$  value from the cumulative  $t$  distribution:

$$p(t) = \frac{B\left(\frac{t + \sqrt{t^2 + n}}{2\sqrt{t^2 + n}}, \frac{n}{2}, \frac{n}{2}\right)}{B\left(\frac{n}{2}, \frac{n}{2}\right)} \quad (36)$$

where  $B$  is the Beta function. Eq. 36 is solved with Brent's method of bisection (Press et al., 1996). After the  $t$ -test, model results are normalized to experimental data. By substituting  $C_d/davg$  into eq. 30 an average model density  $\rho_{f,mod}$  is obtained. Next, the settling velocity of the particles calculated with  $d_{mod}$  and the experimental  $d$  are equated:

$$\frac{4gd(\rho_s - \rho_{f,norm})}{3C_d\rho_{f,norm}} = \frac{4gd_{mod}(\rho_s - \rho_{f,mod})}{3C_d\rho_{f,mod}} \quad (37)$$

In (37) the only unknown is  $\rho_{f,norm}$ , which is the flow density normalized to the experimental data. This density is substituted in (30) to get the normalized ratio  $C_d/dnorm$  that is in turn used in eq. 30 to get the normalized squared shear velocity  $u_{* norm}^2$ . The shear stress associated to  $u_{* norm}^2$  and  $\rho_{f,norm}$  are then used in (9) to calculate the average value of the shear stress  $\tau_{avg}$ . It is to note that the *norm* value are considered as representative of the average solution (*avg* hereafter).

Once the average values of shear velocity, flow density and shear stress are known, PYFLOW defines an interval of variation equal to  $\pm 1$  unit of standard deviation around the average, corresponding to the maximum and minimum acceptable model solutions, respectively. In a Gaussian distribution the range enclosed in this interval corresponds to a probability of 68%, 34%

on the left and 34% on the right of the average. This range is considered as covering a significant spectrum of model solutions for the obtainment of a statistic range of impact parameters to be used for hazard assessment. By using this standard, PYFLOW calculates the interval by subdividing the total area subtended by the function of  $C_d/d$  vs.  $u_*^2$  into two parts, one on the left and one on the right side of the average value. If one assigns to each part 100% of probability and calculates the total area on that part with the following equation:

$$\frac{C_d}{d} = \int_{u_*^2=100kg/m^3}^{u_*^2=avg} \frac{4g \left( \rho_s - \frac{\theta g d_1 \rho_{s1}}{u_*^2 + \theta g d_1} \right)}{3u_*^2 \left( \frac{\theta g d_1 \rho_{s1}}{u_*^2 + \theta g d_1} \right)} du_*^2 \quad (38)$$

it turns out that 68% of this quantity represents the  $C_d/d$  value corresponding to 34% of the probability to the left of the average,  $C_d/d_{left}$ . With the same approach the right value  $C_d/d_{right}$  is calculated. Upon substituting  $C_d/d_{left}$  and  $C_d/d_{right}$  in eq. 31 the corresponding squared shear velocities, i.e.  $u_{*min}^2$  and  $u_{*max}^2$  respectively, are obtained. Again, Brent's method of bisection is used for solving this non-linear equation. Using these values together with the corresponding  $C_d/d$  values, the associated minimum and maximum densities ( $\rho_{f,min}$  and  $\rho_{f,max}$ ) and the minimum and maximum shear stresses ( $\tau_{min}$  and  $\tau_{max}$ ).

## 2.5. Two-components model

---

As previously stated, the complete sequence of layers involving both the coarse particles moved at the base (which are generally found in proximal locations, Dellino et al. (2008)), and the overlying laminated layer can be not found in the deposit stratigraphy. Frequently, the coarse layer (A in fig. 1b) is lacking from the bed-set (especially in distal localities), thus preventing the application of the Shield criterion (eq. 5). Anyway it is still possible to apply the model even if only the laminated layer is present (B in fig. 1b). The laminated layer is composed of different types of particles (components) having different densities, grain sizes and shapes. Since all the components in a lamina are deposited at the same flow conditions and the same settling velocity, one may assume that aerodynamic equivalence exists between the different components. By considering, for example, juvenile particles and loose crystals, the following equation can be written:

$$w_{juv} = w_{xx} \quad (39)$$

that leads to:

$$u_*^2 = \frac{4gd_{juv}(\rho_{s,juv} - \rho_f)}{3C_{d,juv}\rho_f} = \frac{4gd_{xx}(\rho_{s,xx} - \rho_f)}{3C_{d,xx}\rho_f} \quad (40)$$

where the subscript *juv* and *xx* refer to juvenile and crystal particles, respectively. By simplifying eq. 40, the ratio  $C_{d,juv}/d_{juv}$  can be obtained:

$$\frac{C_{d,juv}}{d_{juv}} = \frac{C_{d,xx}(\rho_{s,juv} - \rho_f)}{d_{xx}(\rho_{s,xx} - \rho_f)} \quad (41)$$

and an equation of  $C_{d,juv}/d_{juv}$  as a function of  $u_*^2$  is also obtained:

$$\frac{C_{d,juv}}{d_{juv}} = \frac{g \left( \frac{3C_{d,xx}}{gd_{xx}} + \frac{4(\rho_{s,juv} - \rho_f)}{u_*^2} \right)}{3\rho_{s,xx}} \quad (42)$$

Eqs. 41 and 42 play the same role as eqs. 30 and 31 of the two layer method of Section 2.4. The procedure then follows the same steps. It is to note that also lithic components can be used for solving the system of equations, assuming that a careful estimation of their physical characteristics is made, which sometimes is more difficult than for ashy glass grains or crystals, since lithics can show a wider variation of density and shape characteristics. As a general guideline, it is recommended to use juvenile and crystals (of any kind), especially if they show a unimodal grainsize distribution.

## 2.6. Flow stratification model

---

The bulk density of the shear current obtained with any of the two models discussed so far can be seen as the average value of the density profile from the base of the current to the height at which flow density becomes equal to atmospheric density (top of the shear current, i.e., the portion of the DPDC that is denser than atmosphere). The flow bulk density is a function of particle concentration and gas density (eq. 3). From (3), upon assuming a gas density and considering a representative value of  $\rho_s$ , the average particle concentration  $C$  in the shear current is readily obtained for each considered solution of flow bulk density:

$$C_{avg} = \frac{\rho_{f,avg} - \rho_g}{\rho_s - \rho_g} \quad (43a)$$

$$C_{max} = \frac{\rho_{f,max} - \rho_g}{\rho_s - \rho_g} \quad (43b)$$

$$C_{min} = \frac{\rho_{f,min} - \rho_g}{\rho_s - \rho_g} \quad (43c)$$

Currently the model considers the value of the density of the component representative of the laminated layer if the `twolayers` model is applied; if `twocomponents` is used instead, the density of the less dense component is considered. If one assumes that the particle settling rate is constant during the formation of the whole laminated layer, the total height of the flow  $z_{tot}$  can be obtained by the ratio between  $C$  and the laminated layer total thickness  $z_{lam}$ . In this way the average, maximum and minimum solutions of  $z_{tot}$  are calculated. However, assuming a gas density is a strong approximation, since the density of the gas phase in the DPDC can change significantly and quickly along its path due to entrainment of external air and temperature decrease. From version 2.3 a new method has been introduced that treats the gas density as an unknown variable.

PYFLOW allows choosing between two approaches: 1) three-equations method, in which the gas density, the average Rouse number of the particle suspension  $P_{n,susp}$  and total flow thickness are treated as unknown; 2) two-equations method, in which the average Rouse number of the particle suspension  $P_{n,susp}$  and the thickness of the shear flow  $z_{sf}$  are unknown.

### 2.6.1. Three-equations method

---

The shear current is composed of gas and a mixture of particles, in which those with  $P_n = 2.5$  are at settling condition. Finer particles are held in suspension by turbulent stress and contribute to the concentration profile  $C(z)$ , but their average Rouse number  $P_{n,susp}$ , which is lower than 2.5, is unknown. In addition, the thickness of the shear flow  $z_{tot}$  and the flow gas density  $\rho_g$  are unknown. In order to get these three unknowns, a system of three equations can be written:

$$\rho_{atm} = \rho_g + \left( (\rho_s - \rho_g) C_0 \left( \frac{z_0}{z_{tot} - z_0} \frac{z_{tot} - z_{sf}}{z_{sf}} \right)^{P_{n,susp}} \right) \quad (44)$$

$$\rho_f = \frac{1}{z_{sf} - z_0} \int_{z_0}^{z_{sf}} \left[ \rho_g + \left( (\rho_s - \rho_g) C_0 \left( \frac{z_0}{z_{tot} - z_0} \frac{z_{tot} - z}{z} \right)^{P_{n,susp}} \right) \right] dz \quad (45)$$

$$z_{tot} = \frac{z_{lam}}{C} = \frac{z_{lam}}{\frac{\rho_f - \rho_g}{\rho_s - \rho_g}} \quad (46)$$

The first equation states that the atmospheric density is reached at the top of the shear flow  $z_{sf}$ ; the second one defines the average flow density calculated between  $z_0$  and  $z_{sf}$ ; the third equation defines the total flow thickness as the ratio between the thickness of the laminated layer in the deposit and the average concentration in the flow, defined as in (43). To solve this system of equations,  $z_{sf}$  needs to be evaluated first and this can be done by knowing the flow shear stress calculated in the previous step and the slope angle  $\alpha$ :

$$z_{sf} = \frac{\tau}{(\rho_f - \rho_{atm}) g \sin \alpha} \quad (47)$$

The system of equation is solved numerically by PYFLOW using the Newton-Raphson method to obtain the three solutions (average, maximum and minimum) for the gas density  $\rho_g$ ,  $z_0$  and  $z_{tot}$ . This method is activated if the user provides the slope angle  $\alpha$  (SLOPE\_GROUND) and does not provide the gas density (DENGAS) in the input file. From v2.4, the user can activate multiple “ensemble” solutions by varying the slope angle within a range (SLOPE\_GROUND\_MIN to SLOPE\_GROUND\_MAX) with a defined angle step-size (DELTA\_SLOPE). In this way it is possible exploring the uncertainty related to the slope angle, which is a parameter that is both difficult to estimate in the field and critical for the solution.

In some cases the three equations system fails to converge to realistic solutions and this is strongly dependent on the imposed  $z_0$  value. For this reason, the system is solved iteratively by varying  $z_0$  randomly, starting from  $z_0 = z_{lam}$  and decreasing it progressively by subtracting a value equal to  $\varepsilon * z_0$  (where  $\varepsilon$  is set to 0.01 by default and can be changed by the user specifying EPSDZ0) or to the value set by the user. Very often multiple values of  $z_0$  lead to convergence of the system of the

equations. In this case, PYFLOW calculates the average of the obtained solutions for  $P_{n,susp}$ ,  $z_{tot}$  and  $\rho_g$ .

Subsequently, PYFLOW uses  $\rho_g$  to calculate the flow temperature  $T$ , assuming the flow is composed by the solid particles, the magmatic gas and entrained air, if the user provides in input: the temperature of the magmatic gas  $T_m$ , the air temperature (set by default to 293 K if not provided), the temperature of the solid particles  $T_s$ , the specific gas constant of the magmatic gas  $R_m$  and air  $R_a$  (set by default to 287 J kg<sup>-1</sup> K<sup>-1</sup>), the specific heat at constant pressure of the magmatic gas  $Cp_m$  and of the solid particles  $Cp_s$  and the average density of the solid particles  $\rho_s$ . First, the density of the magmatic gas and entrained air by solving for the equation of state:

$$\rho_m = \frac{p_a}{R_a T_a} \quad (48a)$$

$$\rho_a = \frac{p_a}{R_m T_m} \quad (48b)$$

hence, with the assumption that the gas phases are at constant atmospheric pressure  $p_a$  (set to 101325 Pa if not specified in input by the user). From these densities and the flow gas density  $\rho_g$ , one can calculate the relative volumetric concentration of the magmatic gas  $C_{gm,rel}$  and entrained air  $C_{ga,rel}$ :

$$C_{gm,rel} = \frac{\rho_g - \rho_a}{\rho_m - \rho_a} \quad (49a)$$

$$C_{ga,rel} = 1 - C_{gm} \quad (49b)$$

These concentrations are still not the real volumetric concentrations in the multiphase flow that includes the solid particle concentration calculated via eq. (43), hence they need to be rescaled so that the sum of their rescaled values equals  $1 - C$ :

$$C_{gm} = C_{gm,rel}(1 - C) \quad (50a)$$

$$C_{ga} = C_{ga,rel}(1 - C) \quad (50b)$$

Finally, the flow temperature can be calculated using the following equation:

$$T = \frac{\rho_m C_{gm} T_m Cp_m + \rho_a C_{ga} T_a Cp_a + \rho_s C T_s Cp_s}{\rho_m C_{gm} Cp_m + \rho_a C_{ga} Cp_a + \rho_s C Cp_s} \quad (51)$$

### 2.6.2. Two-equations method

In this method, activated when the gas density is provided in input, only the equations (44) and (45) are used in order  $P_{n,susp}$  and  $z_{sf}$ . This system of equation is solved in two different steps:

1. first, by setting  $z_0 = z_{lam}$ , and considering the average solutions of  $z_{tot}$  and  $\rho_f$ , the system is solved to find the average shear flow thickness  $z_{sf,avg}$  and the average solution of the Rouse number  $P_{n,susp,avg}$ . After the average values of the Rouse number and of the shear flow thickness have been determined, by knowing the average shear stress and flow density found

previously, the slope  $\alpha$  of the substrate over which the DPDC was moving can be calculated by inverting equation (47):

$$\sin \alpha = \frac{\tau}{(\rho_f - \rho_{atm})g z_{sf}} \quad (52)$$

2. Once the average values of the shear flow thickness, the Rouse number and the slope are found, from the same system it is possible to calculate the maximum and the minimum solution of  $z_0$  and  $P_{n,susp}$ . For the maximum solutions ( $z_{0,max}$  and  $P_{n,susp,max}$ ), the flow density is set equal to the previously calculated maximum solution  $\rho_{f,max}$ . Then, the corresponding shear flow thickness is calculated by (47). Since at the maximum density corresponds the minimum shear velocity (Dellino et al. 2008),  $\tau = \tau_{min}$  when  $\rho_f = \rho_{f,max}$ . Thus, the shear flow thickness in this case is the minimum value,  $z_{sf,min}$ . In addition, the total flow thickness is set equal to its maximum solution. For the minimum solutions ( $z_{0,min}$  and  $P_{n,susp,min}$ ) the procedure is the same but the opposite values are used.

The atmospheric density is set equal to  $1.22 \text{ kg m}^{-3}$ . For  $\rho_g$ , in the original formulation (Dellino et al. 2008) the density of steam at  $300^\circ\text{C}$  is used, as it is considered as a reasonable value for DPDCs; however, the user is free to set this value in input.

Alternatively, if the user provides the value of the slope in input, step 2 described above is used for finding the average, maximum and minimum solutions of  $z_0$  and  $P_{n,susp}$ , with equation (47) used directly to find the three solutions of  $z_{sf}$ .

### 2.6.3 Vertical profiles of the flow variables

---

It is now possible to create the profiles of the DPDC parameters; for each variable, an average, maximum and minimum solution profile is created. Concentration, density, velocity and dynamic pressure profiles are calculated by using (1), (3) and (4), respectively. The temperature profile is also calculated using equation (51) if the three-equations system is activated. It is now possible to calculate the dynamic pressure profile:

$$P_{dyn}(z) = \frac{1}{2} \rho_f(z) u(z)^2 \quad (53)$$

PYFLOW calculates and stores the profiles  $C(z)$ ,  $u(z)$ ,  $\rho_f(z)$  and  $P_{dyn}(z)$  in separate output files. Furthermore, it calculates specific dynamic pressures at different heights (10 m by default and at user requested heights), i.e. the dynamic pressure averaged over the height:

$$P_{dyn,sp} = \frac{1}{z_{sp} - z_0} \int_{z_0}^{z_{sp}} \frac{1}{2} \rho_f(z) u(z)^2 dz \quad (54)$$

where  $z_{sp}$  is the chosen height. In addition, in this case the parameter is calculated for the average, maximum and minimum solutions. This is an important choice for hazard assessment: the default value of 10 m is typical of small-medium buildings; PYFLOW allows selecting other heights, which can be more suitable for the hazard assessment in a specific area.

## 2.7 Deposition model

---

The deposition model, if invoked with the command DEPRATES = .T., calculates the deposition rate and time from the pyroclastic density current based on the flow (e.g. flow density, shear velocity, etc.) and deposit properties (componentry, grainsize distributions, etc.). Flow properties needed to execute the deposition model (namely density  $\rho_f$ , thickness  $z_{tot}$ , shear velocity  $u_*$ ) come either from the solution of the sedimentological model presented above or from input. The deposition model, in fact, can run as a standalone program (ONLY\_DEPRATES = .T.), provided all the needed flow and particles properties are given in input.

In this model, the deposition rate  $R$  of the  $j^{th}$  grainsize class of a component  $i$  forming the deposit is given by:

$$R_{i,j} = \rho_{s,i,j} w_{i,j} C_{i,j} \quad (55)$$

where  $C_{i,j}$  is the particle volumetric concentration of each grainsize class  $j$  in the flow. Since particle density  $\rho_{s,i,j}$  is an input parameter and the terminal velocity  $w_{i,j}$  can be readily calculated by eq. (7),  $C_{i,j}$  need to be evaluated at this stage. A distinction between the deposition from turbulent suspension and that from the wash load is made. Each grainsize class is assigned to one of the two categories based on its Rouse number  $P_{n,i,j}$ :

|                      |                         |
|----------------------|-------------------------|
| Wash-load            | $P_{n,i,j} < 0.8$       |
| Turbulent suspension | $0.8 < P_{n,i,j} < 5.0$ |
| Fall                 | $P_{n,i,j} > 5.0$       |

Particles whose Rouse number is less than 0.8 constitute the wash load, the part of particles that are uniformly distributed throughout the flow and mainly settle in the waning stage of the flow. If a fine massive layer is observed in the deposit (level C in fig. 1a), PYFLOW can calculate the deposition rate and time contributions of this layer if the layer thickness is provided ( $z_{lam, massive}$ ). In the current version, PYFLOW automatically assumes this layer is formed by particles of the wash-load ( $P_{n,i,j} < 0.8$ ). If a grainsize and componentry analysis of this specific layer is carried out, it is possible to calculate the deposition rate and time only of this layer separately given the capability of PYFLOW to run this module as a standalone. Additionally, particles with a Rouse number greater than 5 can be optionally discarded with the command PN\_CUT = .T., since these particle can be considered to fall in the deposit without being really influenced by the turbulent flow.

The deposition model goes through the following steps:

- 1) If wanted by the user, the model groups adjacent grainsize classes when  $p_{s,i,j} < tol$ , where  $tol$  is the merging tolerance provided in the `input.dat` file with the command SENSERGE.
- 2) The terminal velocity of each grainsize class  $w_{i,j}$  and hence the Rouse number  $P_{n,i,j}$  are calculated. This step is important for distinguish the grainsize classes of the suspension load from those of the wash load. Particles whose Rouse number is larger than 5 can be excluded from the calculation from this stage on.

3) The particle volumetric concentration at deposition of the grainsize classes forming the turbulent suspension is calculated using the model of Dellino et al. (2019a), who obtained a model for the deposition rate from turbulent boundary layer shear flows from large-scale experiments. The equation for  $C_{i,j}$  is:

$$C_{i,j} = \frac{\frac{p_{s,i,j}/\rho_{s,i,j}}{\sum_{i=1}^{n_{comp}} \sum_{j=j_{wash,i}+1}^{n_{classes,i}} p_{s,i,j}/\rho_{s,i,j}} * C_{tot}}{\left( \left( 10.065 * \frac{P_{n,i,j}}{P_n^*} \right) + 0.1579 \right)} * 0.7 + \frac{\frac{p_{s,i,j+1}/\rho_{s,i,j+1}}{\sum_{i=1}^{n_{comp}} \sum_{j=j_{wash,i}+1}^{n_{classes,i}} p_{s,i,j}/\rho_{s,i,j}} * C_{tot}}{\left( \left( 10.065 * \frac{P_{n,i,j+1}}{P_n^*} \right) + 0.1579 \right)} * 0.3 \quad (56)$$

Where  $C_{tot}$  is the average total volumetric concentration of particles in the flow:

$$C_{tot} = \frac{\rho_f - \rho_g}{\sum_{i=1}^{n_{comp}} \sum_{j=j_{wash,i}+1}^{n_{classes,i}} \rho_{s,i,j} w_{i,j} C_{i,j}} \quad (57)$$

$P_n^*$  is the normalized flow Rouse number, given by:

$$P_n^* = \frac{\sum_{i=1}^{n_{comp}} \sum_{j=j_{wash,i}+1}^{n_{classes,i}} P_{n,i,j} \frac{p_{s,i,j}/\rho_{s,i,j}}{\sum_{i=1}^{n_{comp}} \sum_{j=j_{wash,i}+1}^{n_{classes,i}} p_{s,i,j}/\rho_{s,i,j}} * C_{tot}}{\sum_{i=1}^{n_{comp}} \sum_{j=j_{wash,i}+1}^{n_{classes,i}} p_{s,i,j} \rho_{s,i,j}} \quad (58)$$

and  $j_{wash,i}$  is the index of the coarsest grainsize class constituting the wash load for the  $i^{th}$  component.

4) If the fine massive layer is taken into account for calculations, for each grainsize class of the wash load ( $P_{n,i,j} < 0.8$ ) particle volumetric concentration is calculated by assuming that these particles settle at a constant deposition rate and were uniformly distributed along the flow thickness. In this way one can estimate the particle volumetric concentration by the ratio between the layer thickness (the portion of the deposit that can be attributed to the  $j^{th}$  grainsize class of the  $i^{th}$  component) and flow thickness:

$$C_{i,j} = \frac{p_{s,i,j,massive} z_{lam,massive}}{z_{tot}} \quad (59)$$

In this equation,  $p_{s,i,j,massive}$  is the weight fraction of the grainsize classes in the fine massive layer, recalculated with the assumption that componentry and grainsize distributions are the same as the particles constituting the laminated layer, the model first calculate the weight fractions of the grainsize classes in the fine massive layer:

$$p_{s,i,j,massive} = p_{s,j} \frac{p_{s,tot,wash}}{p_{s,tot}} \quad (60)$$

Where  $p_{s,tot,wash}$  is the sum of the weight fractions of all the grainsize classes constituting the wash load,  $p_{s,tot,wash}$  is the sum of all weight fractions. The flow density considering only the wash load  $\rho_{f,wash}$ , which represents the density of the flow in its waning stage, is also calculated:

$$\rho_{f,wash} = \sum_{i=1}^{n_{comp}} \sum_{j=1}^{j_{wash,i}} C_{i,j,massive} \rho_{s,i,j} + \left( 1 - \sum_{i=1}^{n_{comp}} \sum_{j=1}^{j_{wash,i}} C_{i,j,massive} \right) \rho_{atm} \quad (61)$$

This is needed for calculating the terminal velocity of particles forming the fine massive layer  $w_{i,j,massive}$ , which were settling in a flow of density  $\rho_{f,wash}$  instead of  $\rho_f$ .

6) The deposition rate from turbulent suspension and wash load forming the fine massive layer (if present) are finally calculated:

$$R_{tot,susp} = \sum_{i=1}^{n_{comp}} \sum_{j=j_{wash,i+1}}^{n_{classes,i}} \rho_{s,i,j} w_{i,j} C_{i,j} = \sum_{i=1}^{n_{comp}} \sum_{j=j_{wash}+1}^{n_{classes,i}} R_{i,j,susp} \quad (62)$$

$$R_{tot,massive} = \sum_{i=1}^{n_{comp}} \sum_{j=1}^{j_{wash,i}} \rho_{s,i,j} w_{i,j} C_{i,j} = \sum_{i=1}^{n_{comp}} \sum_{j=1}^{j_{wash,i}} R_{i,j,massive} \quad (63)$$

$$R_{tot} = R_{tot,susp} + R_{tot,massive} \quad (64)$$

7) The corresponding deposition times are finally calculated:

$$t_{dep,susp} = \frac{z_{lam,susp} C_0 \sum_{i=1}^{n_{comp}} \sum_{j=j_{wash,i+1}}^{n_{classes,i}} \rho_{s,i,j} p_{s,i,j}}{R_{tot,susp}} \quad (65)$$

$$t_{dep,massive} = \frac{z_{lam,massive} C_0 \sum_{i=1}^{n_{comp}} \sum_{j=1}^{j_{wash,i}} \rho_{s,i,j} p_{s,i,j}}{R_{tot,massive}} \quad (66)$$

$$t_{dep,tot} = t_{dep,susp} + t_{dep,massive} \quad (67)$$

8) In the new version, a parameter allowing the discrimination between the tractive and massive sedimentation regime is calculated, based on the model presented in Dellino et al. (2019a). This parameter, *STR* (Sedimentation Traction Ratio), is defined as:

$$STR = \frac{S_{rw}}{Q_b} = \frac{A_r \frac{Ref_a}{Ref_w}}{\sum_{i=1}^{n_{comp}} \sum_{j=1}^{n_{classes,i}} q_{b,i,j}} \quad (68)$$

Where  $S_{rw}$  is the volumetric sedimentation rate per unit width,  $Q_b$  is the total bedload transportation rate obtaining by summing all the bedload transportation rates of each grainsize class  $i$  of each component  $j$   $q_{b,i,j}$ ,  $A_r$  is the deposit accretion rate given by the ratio between the total sedimentation rate and the bulk density of the deposit,  $Ref_a$  and  $Ref_w$  are a reference area and width, respectively

(taken as  $1 \text{ m}^2$  and  $1 \text{ m}$  in PYFLOW v2.2 and later versions following Dellino et al. (2019a)). The bedload transportation rates  $q_{b,i,j}$  are calculated as:

$$q_{b,i,j} = W_{i,j}^* \frac{p_{s,i,j} u_*^3}{\left(\frac{\rho_{s,i,j}}{\rho_f} - 1\right) g} \quad (69)$$

where:

$$W_{i,j}^* = \begin{cases} 0.002\xi_{i,j}^{7.5} & \text{for } \xi_{i,j} < 1.35 \\ 14\left(1 - \frac{0.894}{\xi_{i,j}^{0.5}}\right) & \text{for } \xi_{i,j} \geq 1.35 \end{cases} \quad (70)$$

$$\xi_{i,j} = \frac{\tau}{\tau_{r,i,j}} = \frac{\tau}{\tau_{rsm} \left(\frac{d_{i,j}}{d_{dep,median}}\right)^{b_{i,j}}} \quad (71)$$

$$b_{i,j} = \frac{0.67}{1 + e^{\frac{1.5 - \frac{d_{i,j}}{d_{dep,median}}}{0.67}}} \quad (72)$$

$$\tau_{rsm} = 0.75\theta_{dep,median} d_{dep,median} g (\rho_{dep,median} - \rho_f) \quad (73)$$

$d_{dep,median}$  and  $\rho_{dep,median}$  are the dimension and density of the median grainsize in the deposit, respectively. This are provided in input by the user via the command DEP\_MEDIAN and RHOS\_MEDIAN (see [keyword table](#)).

A threshold value  $STR=100$  was proposed by Dellino et al. (2019a), namely the regime is tractive when  $STR < 100$ , massive otherwise.

## 2.8. Probability functions of the impact parameters

---

For each fluid dynamic variable of the DPDC, PYFLOW calculates three solutions: average (corresponding to the 50th percentile), maximum (84<sup>th</sup> percentile) and minimum (16<sup>th</sup> percentile). From these values, it builds probability functions with the aim to calculate, for each studied DPDC, the value of the variable (e.g. dynamic pressure, particle concentration at a specific height, rate and time of deposition, etc.) at the percentile of interest.

As a reference probability distribution, PYFLOW employs the Gaussian distribution:

$$f(y) = \frac{1}{\sigma\sqrt{2\pi}} e^{-\frac{(y-\mu)^2}{2\sigma^2}} \quad (74)$$

where  $\sigma$  is the standard deviation and  $\mu$  is the median of a random variable  $y$ . This choice is based both on the fact that the general model starts from a statistical test (see the Student-t test explained in section 2.4) on grain size data, which generally show a Gaussian tendency when expressed in phi units, and also that generally continuous (random) physical variables show a Gaussian tendency. In order to allow the variables solution distribution to conform to the standardized Gaussian distribution, first the 84<sup>th</sup> ( $\mu+2\sigma$ ) and 16<sup>th</sup> ( $\mu-2\sigma$ ) percentile values were rendered symmetrical

around the mean. By indicating the average, maximum and minimum solutions with  $\mu$ ,  $\max$  and  $\min$ , respectively, the best estimate for the symmetrisation parameter  $ms$  is searched for satisfying the following relationship:

$$(\mu + 2\sigma)^{ms} - \mu^{ms} = \mu^{ms} - (\mu - 2\sigma)^{ms} \quad (75)$$

Eq. 75 has two solutions, among which 0 (the trivial solution) is discarded. PYFLOW then searches for the other solution with Brent's method of bisection (Press et al., 1996). The new symmetrized distribution parameters can be calculated by using  $ms$ :

$$\mu_{simm} = \mu^{ms} \quad (76)$$

$$\sigma_{simm} = (\mu + 2\sigma)^{ms} - \mu^{ms} = \mu^{ms} - (\mu - 2\sigma)^{ms} \quad (77)$$

where  $\mu_{simm}$  and  $\sigma_{simm}$  are the median and the standard deviation of the symmetrized probability function, respectively. Using these parameters it is possible to calculate the variable value  $y$  linked to a desired probability  $P(y)$  via the standardized normal distribution  $Z$  ( $\mu = 0$ ,  $\sigma = 1$ ). Indeed, given a probability, the corresponding standardized variable  $Z_{std}$  is readily obtained by the tabulated values. Actually, PYFLOW uses the cumulative distribution function for the  $Z$  distribution:

$$P(Z_{std}) = \frac{1}{2} \left( 1 + \operatorname{erf} \left( \frac{Z_{std}}{2} \right) \right) \quad (78)$$

Once  $Z_{std}$  is found (again by using the Brent's method), and given the definition of a standardized variable:

$$Z_{std} = \frac{y - \mu_{simm}}{\sigma_{simm}} \quad (79)$$

the value of the variable is readily obtained:

$$y = \mu_{simm} + \sigma_{simm} Z_{std} \quad (80)$$

The output of PYFLOW provides the symmetrisation parameter  $ms$ ,  $\mu_{simm}$  and  $\sigma_{simm}$  for each variable. Then it gives out the variables values at the desired probabilities, which the user provides in the command line when requested.

### 3. Solution algorithm

---

PYFLOW is structured in different, separate, subroutines called by the main program `main`. The basic program structure is shown in Fig. 2:

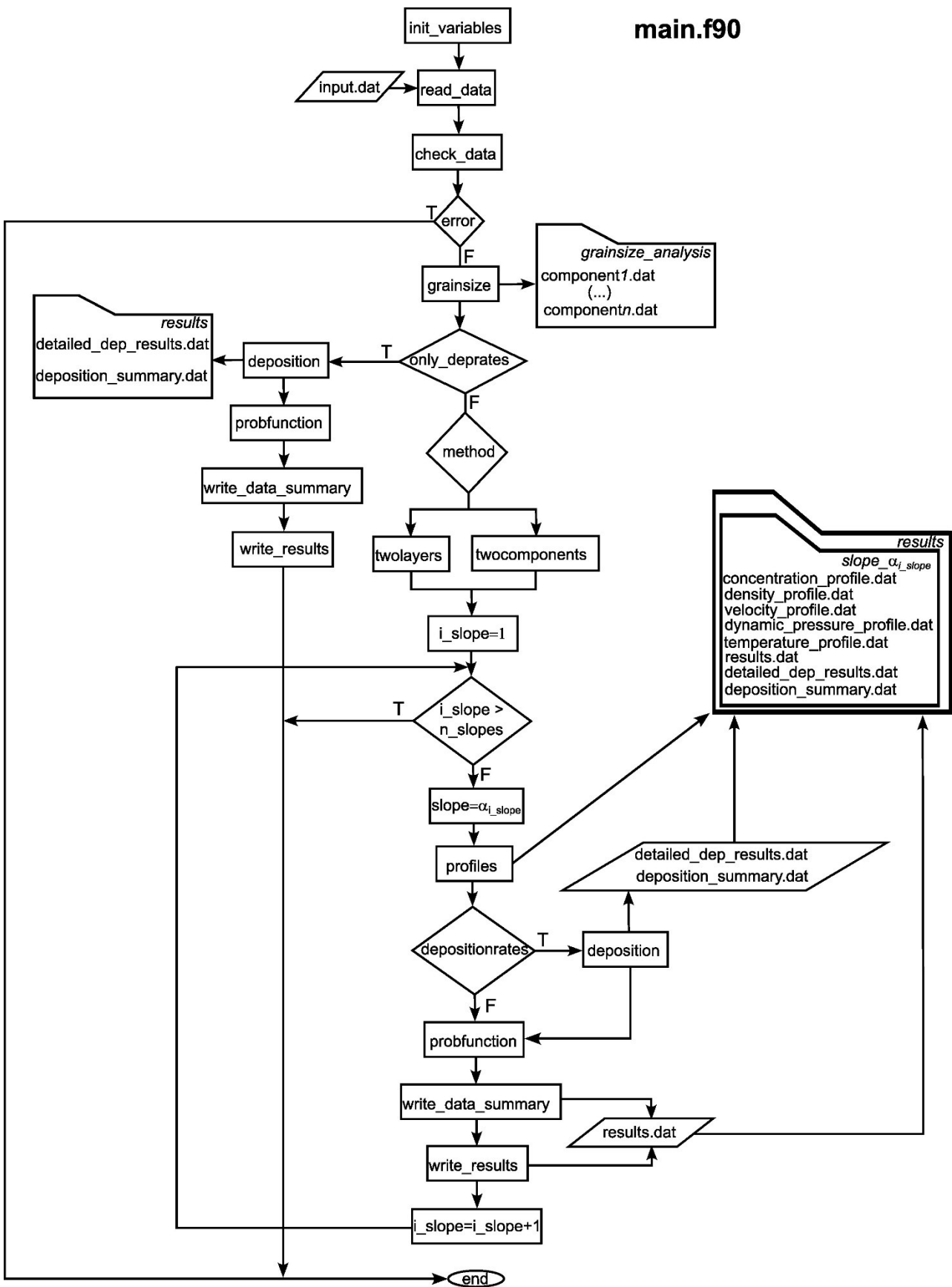


**Figure 2.** Flowchart of PYFLOW\_2.5

PYFLOW is structured in different, separate, subroutines invoked by the main program `main`. The main routine runs the execution of PYFLOW: first it initializes all the variables, then it calls the

subroutine for reading the input data from `input.dat` file; subsequently, it invokes the routine `check_data`, which checks for the completeness and correctness of the input data provided by the user, in agreement with the selected solution model. Data are provided in `input` as a list of assignments commands in the `input.dat` file; the list of all possible commands is included in Table 2. Every missing or wrong inputs generates a fatal error message, with the explanation of the error displayed on the screen and stored into `log.txt`. In case of errors at this stage, the execution stops. Otherwise, the execution proceeds with the routine `init_slopes`, which creates the array of ground slopes to be used in the simulation (one single value or a range of values, see Section 2.6). This is needed at this stage because:

- The routine `outputs` create the folder `results` to store all the simulation outputs; if multiple slopes are requested, hence the simulation runs in ensemble mode, then subfolders called `slope_“slope angle”` are created to store the results of each ensemble simulation;
- In case of ensemble simulations, main loops across the slope values to repeat all the subsequent steps of the simulation until the end.

Subsequently the routine `grainsize` is executed. This routine processes the input data concerning the grainsize data of the components selected for the calculations, for example calculating the median in phi units (if it's provided in mm) and vice versa, performing the grainsize distribution analysis if requested by the user, etc. (see Section 2.3.3). Depending on the user's choice (i.e. available data), PYFLOW proceeds with calling the routine `twolayer` or `twocomponent` (see Section 2.4 and 2.5, respectively), which are followed by the execution of `profiles` (Section 2.6) that calculates the vertical profile of the fluid-dynamic variables (dynamic pressure, velocity, etc.) and writes the results in the corresponding data files (`concentration_profile.dat`, `density_profile.dat`, `velocity_profile.dat`, `dynamic_pressure_profile.dat` and `temperature_profile.dat` if the flow temperature option is activated). From this routine onwards, the execution proceeds in a loop of slope angles until the end, if more than one slope angle is specified. If the user decides to perform the calculations of deposition rate and time, PYFLOW runs the subroutine `deposition` (Section 2.7); as previously introduced, PYFLOW can run this routine as a standalone, in which case the execution jumps from `grainsize` to `deposition` directly. Detailed results from `deposition` (e.g. the deposition rate of all the grainsize classes) are written in separate files (`detailed_dep_results.dat` and `deposition_summary.dat`), which will be analyzed in detail in Section 4.2.3. After this step, the routine `probfunction` is invoked for defining the probability functions as explained in Section 2.8. Finally, PYFLOW writes a summary of input data (with the subroutine `write_data_summary`) and all the main results (with the subroutine `write_results`) in `results.dat`.

There are other external routines invoked during execution. The routine `ttest` performs the t-Student test of the model solution (Section 2.1); `qsimp` calculates numerically the definite integral of a function with the trapezoidal rule (Press et al., 1996), which is used many times in the program; `zbrent` and `rtfslp` are functions that solve for the non-linear equations (e.g. eq. 28) via the Brent's and the false position method, respectively, (Press et al., 1996), invoked many times in `grainsize`, `ttest`, `twolayer`, `twocomponent` and `probfunction` routines. `newt` is the routine that solves the system of non-linear equations (44) - (45) with the Newton-Raphson iterative

method (Press et al., 1996); this routine uses also the module `fminln`. `cd_calculators` contains the functions for calculating the shape-dependent drag coefficients (Section 2.3.1). Other modules are necessary for compiling and running PYFLOW. `inoutdata` stores the used constants (e.g. gravitational acceleration, gas viscosity, etc.), model parameters and defines the variables for the model calculations. The modules `nrtype`, `nrutil` and `nr` are available in the literature (Press et al., 1996) and invoked from the numerical recipes routines (e.g. `newt`); they define data types and store libraries of functions.

A log file `log.txt` is created by PYFLOW for storing all the temporary results and calculation residuals whenever numerical methods are used (see Section 4.2.2).

## 4. Program setup and execution

---

### 4.1. Installation

---

The package comes with all the routines presented in the previous section, each one in a separate `.f90` file. The user needs to compile the FORTRAN90 files and build the executable. In order to simplify this operation, a script (named `Makefile`) is also provided. The script can be invoked with the freeware Gnu Make software. The user should only run the Make program in the folder in which all the source files and the script are stored by typing `make`. The command `make clean` deletes some files created during the compilation: `.mod` and `.o`.

#### 4.1.1. Linux

---

In Linux operating systems Make should be installed by default, otherwise the user can download and install the program with the package manager specific of the OS or by typing the proper command on the command shell (e.g. `apt-get install` for Ubuntu, `yum` for Fedora, etc.). The command `which make` gives information on whether and where Make is installed.

The `Makefile` is written assuming that Gfortran compiler is used. If this is not the case, the user can edit the second line of the `Makefile` by replacing "gfortran" with the proper command invoking the desired compiler.

#### 4.1.2. Windows and Mac OS

---

For Windows and Mac operating systems the user can find the `make` executable on Internet (e.g. [Make for Windows](#)). For these OSs only the executable is available, which has to be placed in the same folder where the `Makefile` script and the source code are. The other possibility is to work with a Linux emulator (e.g. Cygwin for Windows).

## **4.2. Execution**

---

The compilation creates the executable file `pyflow_2.5.exe`, which should be copied in the working folder where `input.dat` file is stored. The execution is launched by typing the proper command on the command prompt (`./pyflow_2.5.exe` for Linux or Linux emulators for Windows and Mac OS, `pyflow_2.5.exe` or simply `pyflow` in the Windows command prompt).

### **4.2.1. The input file**

---

The `input.dat` file should contain a list of keywords that represents variables names and values. The [keywords table](#) lists all the possible keywords with default values (if any), type of the variable, description, model to which the keyword refers, valid values and units. An example of an input file is shown in fig. 3:

```

! Run control data
MU=2.d-5
DENGAS=0.38
MODEL = 'TWOCOMPONENTS'
PROBT = 0.05
ZLAM = 0.58
C0 = 0.75
KS = 0.01
DISTR1 = .T.
DISTR2 = .T.
DEPRATES = .T.
PN_CUT = .T.
NCOMP = 4
INPUT_WEIGHT='MASS'
DEP_MEDIAN=0.000841468
RHOS_MEDIAN=1881.990269
USR_Z_DYNPR = .T.
ZDYNPR(1) = 2
ZDYNPR(2) = 5
USR_PCX_SOL| = .T.
PCX(1) = 0.95

! Component 1 section
RHOLAW(1) = 'POLLENA'
CDLAW(1) = 'DIOGMELE'
SHAPEFACT(1,0) = 0.520
DOTESTCHI(1)=.T.
SIGLEVCHI(1)=0.05
DAVGEQSPH(1)=0.143
PHIMIN(1)=-2.5
PHIMAX(1)=6.5
DPHI(1)=0.5
WEIGHT(1,1)=15.1
WEIGHT(1,2)=26.6
WEIGHT(1,3)=30.4
WEIGHT(1,4)=27.2
WEIGHT(1,5)=16.5

```

**Figure 3.** Example of an `input.dat` file.

In the example, a test case using the Two-components model (Section 2.5) is shown. It is to note that all lines starting with “!” are ignored by the program according to the FORTRAN standard. Therefore the headings (e.g. “Component 1 section”) are not needed and serve as a guidance for the reader. In this particular example, the two components are represented by juvenile particles (with a median size of 1.575 mm, sorting 1.52  $\varphi$ , representative density of  $1228 \text{ kg m}^{-3}$ ) and crystals (with a median size of 0.45 mm, sorting 1.93  $\varphi$ , representative density of  $2425 \text{ kg m}^{-3}$ ). For each parameter, the first index in bracket represent the component number and the second the grainsize class number, with “0” representing the median grainsize. In both case, the Dellino et al. (2005) model is chosen for calculating the shape-dependent drag (Table 1), hence the shape factor  $\Psi$  needs to be specified, being 0.4 and 0.607 for the first and the second component, respectively. The layer thickness is 0.22 m. As specified in the `input.dat` files, the dynamic pressure at 5 and 2 m will

be provided in output; finally, for each computed parameter values of the solutions at 95<sup>th</sup> and 99<sup>th</sup> percentile will also be displayed and saved in the `results.dat` file (Section 2.8). The command “ZOMINGUESS” is not mandatory but in some cases requested for solving the system of equations 43-44 (Section 2.6), when the Newton method fails to converge to a solution for the maximum and the minimum values of  $z_0$  and  $P_{n,susp}$ ; in this case PYFLOW displays a message on the terminal (and in the `log.txt` file) requesting to change the initial guess of  $z_0$  (which by default is  $10^{-4}$  m).

As explained above, PYFLOW gives the possibility to compute the central tendency parameters (median and sorting) of the component by activating the grainsize distribution analysis by setting DISTR1 and/or DISTR2 (for the first and/or the second component) to .TRUE. (Section 2.3). In this case, the weights (INPUT\_WEIGHT = ‘MASS’) or the weight fractions (INPUT\_WEIGHT = ‘WT’) of each grainsize class for each component must be provided in the input file, as shown in fig. 4:

```

! Component 1 section
RHOLAW(1) = 'POLLENA'
CDLAW(1) = 'DIOGMELE'
SHAPEFACT(1,0) = 0.520
DOTESTCHI(1)=.T.
SIGLEVCHI(1)=0.05
DAVGEQSPH(1)=0.143
PHIMIN(1)=-2.5
PHIMAX(1)=6.5
DPHI(1)=0.5
WEIGHT(1,1)=15.1
WEIGHT(1,2)=26.6
WEIGHT(1,3)=30.4
WEIGHT(1,4)=27.2
WEIGHT(1,5)=16.5
WEIGHT(1,6)=28.85
WEIGHT(1,7)=30.38
WEIGHT(1,8)=28.35
WEIGHT(1,9)=32.09
WEIGHT(1,10)=26.16
WEIGHT(1,11)=20.37
WEIGHT(1,12)=12.98
WEIGHT(1,13)=14.37
WEIGHT(1,14)=7.58
WEIGHT(1,15)=5.72
WEIGHT(1,16)=3.05
WEIGHT(1,17)=2.13
WEIGHT(1,18)=1.21
WEIGHT(1,19)=0.44

! Component 2 section
RHOLAW(2) = 'CUSTOM'
RHO_CUSTOM(2) = 'CONSTANT'
RHOS(2,0) = 3280
CDLAW(2) = 'DIOGMELE'
SHAPEFACT(2,0) = 0.610
DOTESTCHI(2)=.T.
SIGLEVCHI(2)=0.05
PHIMIN(2)=-1.0
PHIMAX(2)=6.5
DPHI(2)=0.5
WEIGHT(2,1)=0.71
WEIGHT(2,2)=4.78
WEIGHT(2,3)=8.55
WEIGHT(2,4)=9.61
WEIGHT(2,5)=17.64
WEIGHT(2,6)=21.97
WEIGHT(2,7)=22.51
WEIGHT(2,8)=15.62
WEIGHT(2,9)=10.94
WEIGHT(2,10)=12.12
WEIGHT(2,11)=6.39
WEIGHT(2,12)=4.82
WEIGHT(2,13)=2.57
WEIGHT(2,14)=1.79
WEIGHT(2,15)=1.02
WEIGHT(2,16)=0.37

```

**Figure 4.** Example of a `input.dat` file with weights specified for the grainsize distribution analysis.

Relevant example cases are provided in the software package, it is recommended to start using PYFLOW by amending the `input.dat` file of the examples.

#### 4.2.2. The log file

---

At runtime, PYFLOW continuously displays error or warning messages, temporary results and residuals of numerical calculations on the terminal. At the end of the execution it is usually not possible to go back to the first output messages, due to the space limitations of the prompt command shell. For this reason, all the output is also stored in a log file, named `log.txt`, which can be examined by the user at any time.

#### **4.2.3. Output files**

---

PYFLOW opens at least the following output files in a new folder called “results”:

- results.dat
- log.txt
- concentration\_profile.dat
- dynamic\_pressure\_profile.dat
- velocity\_profile.dat
- density\_profile.dat

If grainsize distribution analysis is performed for selected or all components, results of this analysis are saved in separate files called component“n”.dat, where “n” is replaced with the number identifying the component (e.g. component2.dat), stored in a new folder called “grainsize\_analysis”. If the flow temperature calculation is activated (see Section 2.6), then also a temperature\_profile.dat file is created. Furthermore, if deposition rate calculations are activated (DEPRATES=.T., Section 2.7), total deposition rates and times are saved in results.dat (fig. 8) and the results for all the individual grainsize classes are saved in a separate file called detailed\_dep\_results.dat (fig. 9). Finally, if multiple slopes are explored as explained in Section 2.6, all the outputs mentioned above are stored in separate folders called “slope\_xx”, where xx is the value of the slope.

results.dat reports a summary of the input data and results from model calculations, the t-Student test, the probability density functions of the impact parameters and all user requested additional outputs. Screenshots of parts of a results.dat file obtained running the test case in fig. 5 are shown in the following figures. In fig. 5 the first part of the results.dat is displayed: an input data summary is followed by 50<sup>th</sup>, 84<sup>th</sup> and 16<sup>th</sup> percentile solutions for the main flow parameters. The screenshot of the second part of the same file is shown in fig. 6; here, results of the t-Student test are also shown together with the user requested outputs (in this case, the depth-averaged dynamic pressure at 5 and 2 m).

```

###PROGRAM PYFLOW 2.5 by Fabio Dioguardi###
Data summary
*****TWO COMPONENT METHOD*****
COMPONENT 1
Particle density (kg/m^3) 3280.000
Particle equivalent diameter of the median size (mm) 0.315
Sorting particle grainsize distribution (phi) 1.395
Classes number particle grainsize distribution (-) 16
Drag law DIOGMELE
Shape factor (-) 0.610

COMPONENT 2
Particle density (kg/m^3) 1857.591
Particle equivalent diameter of the median size (mm) 0.915
Sorting particle grainsize distribution (phi) 2.079
Classes number particle grainsize distribution (-) 19
Drag law DIOGMELE
Shape factor (-) 0.520

OTHER DATA
Significance level t-test (-) 0.050
Layer thickness (m) 0.58000
Particle concentration in the layer (-) 0.750
Substrate roughness (m) 0.01000
Slope ground (deg) 2.987

Results
50th percentile solution flow density (kg/m^3) 13.918
84th percentile solution flow density (kg/m^3) 2.754
16th percentile solution flow density (kg/m^3) 33.442
50th percentile solution viscous sublayer thickness (m) 0.00550
84th percentile solution viscous sublayer thickness (m) 0.00015
16th percentile solution viscous sublayer thickness (m) 0.01304
50th percentile solution total flow thickness (m) 79.567
84th percentile solution total flow thickness (m) 453.675
16th percentile solution total flow thickness (m) 32.581
50th percentile solution shear flow thickness (m) 1.452
84th percentile solution shear flow thickness (m) 11.956
16th percentile solution shear flow thickness (m) 0.569
50th percentile solution shear velocity (m/s) 0.824
84th percentile solution shear velocity (m/s) 1.854
16th percentile solution shear velocity (m/s) 0.530
50th percentile solution velocity shear stress (Pa) 9.439
84th percentile solution velocity shear stress (Pa) 9.471
16th percentile solution velocity shear stress (Pa) 9.382
50th percentile solution suspension Rouse number (-) 1.329
84th percentile solution suspension Rouse number (-) 0.655
16th percentile solution suspension Rouse number (-) 1.959
50th percentile solution 10m depth-averaged dynamic pressure (Pa) 198.717
84th percentile solution 10m depth-averaged dynamic pressure (Pa) 2130.855
16th percentile solution 10m depth-averaged dynamic pressure (Pa) 65.594
50th percentile solution 2m particle concentration (-) .28608E-03
84th percentile solution 2m particle concentration (-) .14543E-02
16th percentile solution 2m particle concentration (-) .34645E-04
50th percentile solution 2m depth-averaged particle concentration (-) .53654E-02
84th percentile solution 2m depth-averaged particle concentration (-) .40946E-02
16th percentile solution 2m depth-averaged particle concentration (-) .50413E-02

```

**Figure 5.** First part of a results.dat file.

```

Test t-Student summary
Significance level      0.025000
Theoretical t value     2.101
Calculated t value     1.217

### User requested outputs ###
z = 2.00
50th percentile solution depth-averaged dynamic pressure (Pa)      584.197
84th percentile solution depth-averaged dynamic pressure (Pa)      3626.972
16th percentile solution depth-averaged dynamic pressure (Pa)      203.560

z = 5.00
50th percentile solution depth-averaged dynamic pressure (Pa)      301.490
84th percentile solution depth-averaged dynamic pressure (Pa)      2674.069
16th percentile solution depth-averaged dynamic pressure (Pa)      98.683

```

**Figure 6.** Second part of a `results.dat` file.

If the deposition rate calculation is performed, an additional section named “DEPOSITION RATE AND TIME CALCULATIONS” is included in `results.dat`, where the total deposition rate and times are reported, together with laminated layer thickness (the part of the layer which originated from the turbulent suspension) and the total particle concentration of turbulent suspension (fig. 7). Since deposition rate calculations can be performed as standalone up to 5 solutions, a subsection is created for each solution. In the default case in which deposition rate calculations are carried out together with the rest of the sedimentological model, three solutions (corresponding to the 50<sup>th</sup>, 84<sup>th</sup> and 16<sup>th</sup> ones of the sedimentological model) are computed by default.

```

###DEPOSITION RATE AND TIME CALCULATIONS
50th percentile solution

*****SUSPENSION LOAD*****
Laminated layer thickness (m) = 0.525E+00
Deposition rate of turbulent suspension (kg m^-2 s^-1) = 0.375E+01
Deposition time of turbulent suspension (s) = 0.264E+03
Total particle concentration of turbulent suspension = 0.538E-02
Total particle concentration of turbulent suspension at deposition = 0.538E-02
Total particle concentration of turbulent suspension remaining at suspension = -0.173E-17

Volumetric sedimentation rate per unit width (m^2 s^-1) = 0.149E-02
Bedload transportation rate per unit width (m^2 s^-1) = 0.521E-02
Srw/Qb ratio (-) = 0.286

84th percentile solution

*****SUSPENSION LOAD*****
Laminated layer thickness (m) = 0.527E+00
Deposition rate of turbulent suspension (kg m^-2 s^-1) = 0.983E-01
Deposition time of turbulent suspension (s) = 0.101E+05
Total particle concentration of turbulent suspension = 0.942E-03
Total particle concentration of turbulent suspension at deposition = 0.942E-03
Total particle concentration of turbulent suspension remaining at suspension = 0.217E-18

Volumetric sedimentation rate per unit width (m^2 s^-1) = 0.390E-04
Bedload transportation rate per unit width (m^2 s^-1) = 0.117E-01
Srw/Qb ratio (-) = 0.003

16th percentile solution

*****SUSPENSION LOAD*****
Laminated layer thickness (m) = 0.525E+00
Deposition rate of turbulent suspension (kg m^-2 s^-1) = 0.847E+01
Deposition time of turbulent suspension (s) = 0.117E+03
Total particle concentration of turbulent suspension = 0.131E-01
Total particle concentration of turbulent suspension at deposition = 0.131E-01
Total particle concentration of turbulent suspension remaining at suspension = 0.000E+00

Volumetric sedimentation rate per unit width (m^2 s^-1) = 0.336E-02
Bedload transportation rate per unit width (m^2 s^-1) = 0.337E-02
Srw/Qb ratio (-) = 1.000

```

**Figure 7.** Third part of a results.dat file.

The section “PROBABILITY FUNCTION” follows, where the probability function parameters for each impact variable (including the user requested ones) are reported. If the user requests solutions at specified percentiles, the file ends with a section called “FUNCTION VALUES AT USER REQUESTED PERCENTILES”, which lists the values of the impact parameters at user requested percentiles (or exceedance probability).

```

##### PROBABILITY FUNCTIONS #####
10 m dynamic pressure probability function
Symmetrization exponent -0.459
Median 0.88035E-01
Standard deviation 0.58419E-01

2 m particle concentration probability function
Symmetrization exponent 0.141
Median 0.31772E+00
Standard deviation 0.81562E-01

2 m depth-averaged particle concentration probability function
Symmetrization exponent 10.000
Median 0.19770E-22
Standard deviation 0.91674E-23

Flow density probability function
Symmetrization exponent 0.508
Median 0.38083E+01
Standard deviation 0.21355E+01

Flow shear velocity probability function
Symmetrization exponent -1.004
Median 0.12152E+01
Standard deviation 0.67707E+00

2.00 m dynamic pressure probability function
Symmetrization exponent -0.391
Median 0.82760E-01
Standard deviation 0.42243E-01

5.00 m dynamic pressure probability function
Symmetrization exponent -0.422
Median 0.89991E-01
Standard deviation 0.54152E-01

Rtot probability function
Symmetrization exponent 0.819
Median 0.29501E+01
Standard deviation 0.28004E+01

tdep probability function
Symmetrization exponent -0.819
Median 0.10389E-01
Standard deviation 0.98637E-02

```

**Figure 8.** Section of a results.dat file with deposition rate calculation results.

In case of deposition rate and time calculation, a detailed\_dep\_results.dat is created for storing the relevant outputs for all the grainsize classes contributing to the total deposition rate (fig. 9).

```

| *****DEPOSITION RATES AND TIMES CALCULATION*****
### 50th percentile solution ####
Input data summary
Total weight fraction = 0.905
Normalized layer thickness = 0.525
Gas density (kg/m^3) = 0.380
Flow density (kg/m^3) = 13.918
Total particle concentration = 0.538E-02
Flow shear velocity (m/s) = 0.824
Flow total thickness (m) = 79.567

*** Component 1 ***
SUSPENSION LOAD
Class n. = 1
Rate of deposition (kg m^-2 s^-1) = 0.909E-01
Particle concentration = 0.344E-04
Particle terminal velocity (m s^-1) = 1.752
Particle Rouse number = 5.189

Class n. = 2
Rate of deposition (kg m^-2 s^-1) = 0.813E-01
Particle concentration = 0.327E-04
Particle terminal velocity (m s^-1) = 1.541
Particle Rouse number = 4.564

Class n. = 3
Rate of deposition (kg m^-2 s^-1) = 0.493E-01
Particle concentration = 0.217E-04
Particle terminal velocity (m s^-1) = 1.318
Particle Rouse number = 3.904

Class n. = 4
Rate of deposition (kg m^-2 s^-1) = 0.862E-01
Particle concentration = 0.429E-04
Particle terminal velocity (m s^-1) = 1.099
Particle Rouse number = 3.256

Class n. = 5
Rate of deposition (kg m^-2 s^-1) = 0.908E-01
Particle concentration = 0.521E-04
Particle terminal velocity (m s^-1) = 0.899
Particle Rouse number = 2.663

Class n. = 6
Rate of deposition (kg m^-2 s^-1) = 0.847E-01
Particle concentration = 0.573E-04
Particle terminal velocity (m s^-1) = 0.723
Particle Rouse number = 2.142

```

**Figure 9.** Screenshot of detailed\_dep\_results.dat file.

Another additional file, deposition\_summary.dat, is created by deposition for storing all the relevant information (particle size, weight fraction, terminal velocity, Rouse number,

concentration, density and deposition rate) for all the grainsize classes. This file is written in a way that it is easily accessible by data processing software (e.g. Excel).

| Solution | Component | Class | dp (m)    | ps (-)    | wt(m s^-1) | Pn (-) | C (-)     | rhos(kg m^-3) | R(kg m^-1 s^-2) |
|----------|-----------|-------|-----------|-----------|------------|--------|-----------|---------------|-----------------|
| 1        | 1         | 1     | 0.283E-02 | 0.242E-01 | 1.7520     | 5.1888 | 0.344E-04 | 1507.687      | 0.909E-01       |
| 1        | 1         | 2     | 0.200E-02 | 0.217E-01 | 1.5411     | 4.5642 | 0.327E-04 | 1615.124      | 0.813E-01       |
| 1        | 1         | 3     | 0.141E-02 | 0.132E-01 | 1.3181     | 3.9038 | 0.217E-04 | 1722.562      | 0.493E-01       |
| 1        | 1         | 4     | 0.100E-02 | 0.230E-01 | 1.0995     | 3.2564 | 0.429E-04 | 1830.000      | 0.862E-01       |
| 1        | 1         | 5     | 0.707E-03 | 0.242E-01 | 0.8991     | 2.6628 | 0.521E-04 | 1937.438      | 0.908E-01       |
| 1        | 1         | 6     | 0.500E-03 | 0.226E-01 | 0.7232     | 2.1421 | 0.573E-04 | 2044.876      | 0.847E-01       |
| 1        | 1         | 7     | 0.354E-03 | 0.256E-01 | 0.5726     | 1.6960 | 0.778E-04 | 2152.313      | 0.959E-01       |
| 1        | 1         | 8     | 0.250E-03 | 0.209E-01 | 0.4452     | 1.3185 | 0.777E-04 | 2259.751      | 0.782E-01       |
| 1        | 1         | 9     | 0.177E-03 | 0.162E-01 | 0.4433     | 1.3128 | 0.580E-04 | 2367.189      | 0.609E-01       |
| 1        | 1         | 10    | 0.125E-03 | 0.103E-01 | 0.3418     | 1.0123 | 0.459E-04 | 2474.627      | 0.388E-01       |
| 1        | 1         | 11    | 0.884E-04 | 0.115E-01 | 0.2337     | 0.6923 | 0.712E-04 | 2582.065      | 0.429E-01       |
| 1        | 1         | 12    | 0.625E-04 | 0.604E-02 | 0.1505     | 0.4458 | 0.560E-04 | 2689.503      | 0.227E-01       |
| 1        | 1         | 13    | 0.442E-04 | 0.456E-02 | 0.0890     | 0.2636 | 0.696E-04 | 2760.000      | 0.171E-01       |
| 1        | 1         | 14    | 0.313E-04 | 0.243E-02 | 0.0472     | 0.1399 | 0.699E-04 | 2760.000      | 0.912E-02       |
| 1        | 1         | 15    | 0.221E-04 | 0.170E-02 | 0.0228     | 0.0677 | 0.101E-03 | 2760.000      | 0.637E-02       |
| 1        | 1         | 16    | 0.156E-04 | 0.965E-03 | 0.0100     | 0.0296 | 0.131E-03 | 2760.000      | 0.362E-02       |
| 1        | 1         | 17    | 0.110E-04 | 0.351E-03 | 0.0038     | 0.0113 | 0.125E-03 | 2760.000      | 0.132E-02       |
| 1        | 2         | 1     | 0.100E-02 | 0.682E-02 | 1.7084     | 5.0598 | 0.456E-05 | 3280.000      | 0.256E-01       |
| 1        | 2         | 2     | 0.707E-03 | 0.766E-02 | 1.3684     | 4.0528 | 0.640E-05 | 3280.000      | 0.287E-01       |
| 1        | 2         | 3     | 0.500E-03 | 0.141E-01 | 1.0751     | 3.1841 | 0.150E-04 | 3280.000      | 0.527E-01       |
| 1        | 2         | 4     | 0.354E-03 | 0.175E-01 | 0.8312     | 2.4617 | 0.241E-04 | 3280.000      | 0.657E-01       |
| 1        | 2         | 5     | 0.250E-03 | 0.179E-01 | 0.6320     | 1.8718 | 0.325E-04 | 3280.000      | 0.673E-01       |
| 1        | 2         | 6     | 0.177E-03 | 0.125E-01 | 0.4707     | 1.3941 | 0.302E-04 | 3280.000      | 0.467E-01       |
| 1        | 2         | 7     | 0.125E-03 | 0.872E-02 | 0.4368     | 1.2937 | 0.228E-04 | 3280.000      | 0.327E-01       |
| 1        | 2         | 8     | 0.884E-04 | 0.966E-02 | 0.2973     | 0.8805 | 0.371E-04 | 3280.000      | 0.362E-01       |
| 1        | 2         | 9     | 0.625E-04 | 0.509E-02 | 0.1916     | 0.5674 | 0.304E-04 | 3280.000      | 0.191E-01       |
| 1        | 2         | 10    | 0.442E-04 | 0.384E-02 | 0.1154     | 0.3419 | 0.380E-04 | 3280.000      | 0.144E-01       |
| 1        | 2         | 11    | 0.313E-04 | 0.205E-02 | 0.0645     | 0.1912 | 0.363E-04 | 3280.000      | 0.768E-02       |
| 1        | 2         | 12    | 0.221E-04 | 0.143E-02 | 0.0335     | 0.0991 | 0.487E-04 | 3280.000      | 0.535E-02       |
| 1        | 2         | 13    | 0.156E-04 | 0.813E-03 | 0.0161     | 0.0477 | 0.577E-04 | 3280.000      | 0.305E-02       |
| 1        | 2         | 14    | 0.110E-04 | 0.295E-03 | 0.0072     | 0.0212 | 0.471E-04 | 3280.000      | 0.111E-02       |
| 1        | 3         | 1     | 0.283E-02 | 0.438E-01 | 1.8738     | 5.5496 | 0.341E-04 | 2570.000      | 0.164E+00       |
| 1        | 3         | 2     | 0.200E-02 | 0.914E-01 | 1.6057     | 4.7556 | 0.830E-04 | 2570.000      | 0.343E+00       |
| 1        | 3         | 3     | 0.141E-02 | 0.949E-01 | 1.3370     | 3.9600 | 0.104E-03 | 2570.000      | 0.356E+00       |
| 1        | 3         | 4     | 0.100E-02 | 0.742E-01 | 1.0853     | 3.2144 | 0.997E-04 | 2570.000      | 0.278E+00       |
| 1        | 3         | 5     | 0.707E-03 | 0.688E-01 | 0.8638     | 2.5583 | 0.116E-03 | 2570.000      | 0.258E+00       |
| 1        | 3         | 6     | 0.500E-03 | 0.591E-01 | 0.6766     | 2.0040 | 0.127E-03 | 2570.000      | 0.222E+00       |
| 1        | 3         | 7     | 0.354E-03 | 0.463E-01 | 0.5218     | 1.5453 | 0.129E-03 | 2570.000      | 0.174E+00       |
| 1        | 3         | 8     | 0.250E-03 | 0.386E-01 | 0.3948     | 1.1694 | 0.143E-03 | 2570.000      | 0.145E+00       |
| 1        | 3         | 9     | 0.177E-03 | 0.269E-01 | 0.4217     | 1.2489 | 0.931E-04 | 2570.000      | 0.101E+00       |
| 1        | 3         | 10    | 0.125E-03 | 0.194E-01 | 0.3221     | 0.9541 | 0.879E-04 | 2570.000      | 0.728E-01       |
| 1        | 3         | 11    | 0.884E-04 | 0.215E-01 | 0.2084     | 0.6173 | 0.151E-03 | 2570.000      | 0.806E-01       |
| 1        | 3         | 12    | 0.625E-04 | 0.113E-01 | 0.1250     | 0.3703 | 0.132E-03 | 2570.000      | 0.425E-01       |
| 1        | 3         | 13    | 0.442E-04 | 0.856E-02 | 0.0681     | 0.2018 | 0.183E-03 | 2570.000      | 0.321E-01       |
| 1        | 3         | 14    | 0.313F-04 | 0.457F-02 | 0.0331     | 0.0981 | 0.201F-03 | 2570.000      | 0.171F-01       |

**Figure 10.** Screenshot of deposition\_summary.dat file.

Grainsize analyses for each component are conducted by the program by default if the deposition rate utility is activated, or if requested by the user. In this case, PYFLOW generates an additional output file for each component (e.g. component1.dat) in the subfolders “grainsize\_analysis”, in which all the details of the grainsize analysis are stored (fig. 11):

```
***** GRAINSIZE DISTRIBUTION PARAMETERS CALCULATION FOR COMPONENT 1 *****
```

| Phi  | d(mm) | Wt.%  | Fr.Cum.Wt | Cum.Wt%  |
|------|-------|-------|-----------|----------|
| -1.0 | 2.000 | 0.50  | 0.0050    | 0.5021   |
| -0.5 | 1.414 | 3.38  | 0.0388    | 3.8823   |
| 0.0  | 1.000 | 6.05  | 0.0993    | 9.9286   |
| 0.5  | 0.707 | 6.80  | 0.1672    | 16.7244  |
| 1.0  | 0.500 | 12.47 | 0.2920    | 29.1988  |
| 1.5  | 0.354 | 15.54 | 0.4474    | 44.7352  |
| 2.0  | 0.250 | 15.92 | 0.6065    | 60.6534  |
| 2.5  | 0.177 | 11.05 | 0.7170    | 71.6993  |
| 3.0  | 0.125 | 7.74  | 0.7944    | 79.4357  |
| 3.5  | 0.088 | 8.57  | 0.8801    | 88.0065  |
| 4.0  | 0.062 | 4.52  | 0.9253    | 92.5253  |
| 4.5  | 0.044 | 3.41  | 0.9593    | 95.9338  |
| 5.0  | 0.031 | 1.82  | 0.9775    | 97.7512  |
| 5.5  | 0.022 | 1.27  | 0.9902    | 99.0170  |
| 6.0  | 0.016 | 0.72  | 0.9974    | 99.7383  |
| 6.5  | 0.011 | 0.26  | 1.0000    | 100.0000 |

```
*****CHI SQUARED TEST*****
```

| ztest | Oj    | Ej    | (Oj-Ej)^2/Ej |
|-------|-------|-------|--------------|
| -1.19 | 9.93  | 11.64 | 0.25         |
| -0.83 | 6.80  | 8.55  | 0.36         |
| -0.48 | 12.47 | 11.50 | 0.08         |
| -0.12 | 15.54 | 13.61 | 0.27         |
| 0.24  | 15.92 | 14.20 | 0.21         |
| 0.60  | 11.05 | 13.03 | 0.30         |
| 0.96  | 7.74  | 10.54 | 0.75         |
| 1.32  | 8.57  | 7.51  | 0.15         |
| 5.00  | 7.93  | 9.41  | 0.23         |

```
Sensitivity = 0.05
Significance = 0.05
Degrees of freedom = 6.0
Chi calculated = 2.61
Chi tabulated = 12.59
```

```
The distribution is not significantly different from a normal standard distribution
COMPONENT 1 GRAINSIZE ANALYSIS RESULTS
```

```
phi50 = 1.66435 d50 (mm) = 0.79500
phi84 = 2.36001 d84 (mm) = 0.19479
phi16 = -1.79771 d16 (mm) = 3.47669
sigma = 1.39505
```

**Figure 11.** Screenshot of component1.dat file.

In the first part, the weight fractions are shown for each grainsize (represented both in phi and mm); additional column for the cumulative weights (both absolute values and percentage) are also written. The “CHI SQUARED TEST” section follows, which lists the relevant outputs of this statistical test ( $Z_{test}$ , observed and expected values, degrees of freedom, the theoretical and calculated values of the  $\chi^2$  variable), with a final statement explaining the result of the test, i.e. whether the grainsize distribution is significantly different from a normal standard distribution or not. Final results of the grainsize analysis (e.g. median, sorting) are stored at the end of the file. Finally, the profiles files are organized in four columns. The first column is the height  $z$  in m, with a step-size of 0.01 m. To each height, the corresponding variable values for the three solutions (50th,

84th, 16th percentile) are written in the next three columns. Here a part of the file `dynamic_pressure_profile.dat` is given as an example:

| Height (m) | 50th percentile dynamic pressure (Pa) | 84th percentile dynamic pressure (Pa) | 16th percentile dynamic pressure (Pa) |
|------------|---------------------------------------|---------------------------------------|---------------------------------------|
| 0.580      | 0.3677E+03                            | 0.3767E+04                            | 0.5582E+02                            |
| 0.590      | 0.3620E+03                            | 0.3745E+04                            | 0.5480E+02                            |
| 0.600      | 0.3565E+03                            | 0.3723E+04                            | 0.5383E+02                            |
| 0.610      | 0.3511E+03                            | 0.3701E+04                            | 0.5290E+02                            |
| 0.620      | 0.3460E+03                            | 0.3680E+04                            | 0.5202E+02                            |
| 0.630      | 0.3410E+03                            | 0.3659E+04                            | 0.5118E+02                            |
| 0.640      | 0.3362E+03                            | 0.3639E+04                            | 0.5037E+02                            |
| 0.650      | 0.3316E+03                            | 0.3619E+04                            | 0.4960E+02                            |
| 0.660      | 0.3271E+03                            | 0.3599E+04                            | 0.4886E+02                            |
| 0.670      | 0.3227E+03                            | 0.3580E+04                            | 0.4815E+02                            |
| 0.680      | 0.3185E+03                            | 0.3562E+04                            | 0.4748E+02                            |
| 0.690      | 0.3144E+03                            | 0.3543E+04                            | 0.4683E+02                            |
| 0.700      | 0.3104E+03                            | 0.3525E+04                            | 0.4621E+02                            |
| 0.710      | 0.3065E+03                            | 0.3508E+04                            | 0.4561E+02                            |
| 0.720      | 0.3028E+03                            | 0.3490E+04                            | 0.4504E+02                            |
| 0.730      | 0.2991E+03                            | 0.3473E+04                            | 0.4449E+02                            |
| 0.740      | 0.2956E+03                            | 0.3456E+04                            | 0.4396E+02                            |
| 0.750      | 0.2922E+03                            | 0.3440E+04                            | 0.4346E+02                            |
| 0.760      | 0.2888E+03                            | 0.3424E+04                            | 0.4297E+02                            |
| 0.770      | 0.2855E+03                            | 0.3408E+04                            | 0.4250E+02                            |
| 0.780      | 0.2824E+03                            | 0.3393E+04                            | 0.4205E+02                            |
| 0.790      | 0.2793E+03                            | 0.3377E+04                            | 0.4161E+02                            |
| 0.800      | 0.2763E+03                            | 0.3362E+04                            | 0.4120E+02                            |
| 0.810      | 0.2734E+03                            | 0.3347E+04                            | 0.4079E+02                            |
| 0.820      | 0.2705E+03                            | 0.3333E+04                            | 0.4041E+02                            |
| 0.830      | 0.2677E+03                            | 0.3318E+04                            | 0.4003E+02                            |
| 0.840      | 0.2650E+03                            | 0.3304E+04                            | 0.3967E+02                            |
| 0.850      | 0.2624E+03                            | 0.3291E+04                            | 0.3932E+02                            |
| 0.860      | 0.2598E+03                            | 0.3277E+04                            | 0.3898E+02                            |

**Fig. 12.** Screenshot of the `dynamic_pressure_profile.dat`.

Usually 50th, 84th and 16th percentiles correspond to the average, maximum and minimum solutions for the dynamic pressure, but this is not always the case, especially in the basal part of the flow and when the t-Student test succeeds only at very low significance levels. Sometimes, at the chosen height, the 84th percentile does not show an higher value than the 50<sup>th</sup> or the 16th percentiles.

The file is organized in a way that it is easy to draw plots variable vs. height with the most used programs (e.g. Microsoft Excel, Grapher, Kaleidagraph, GnuPlot, etc.). An example drawn with Microsoft Excel is shown in fig. 13.

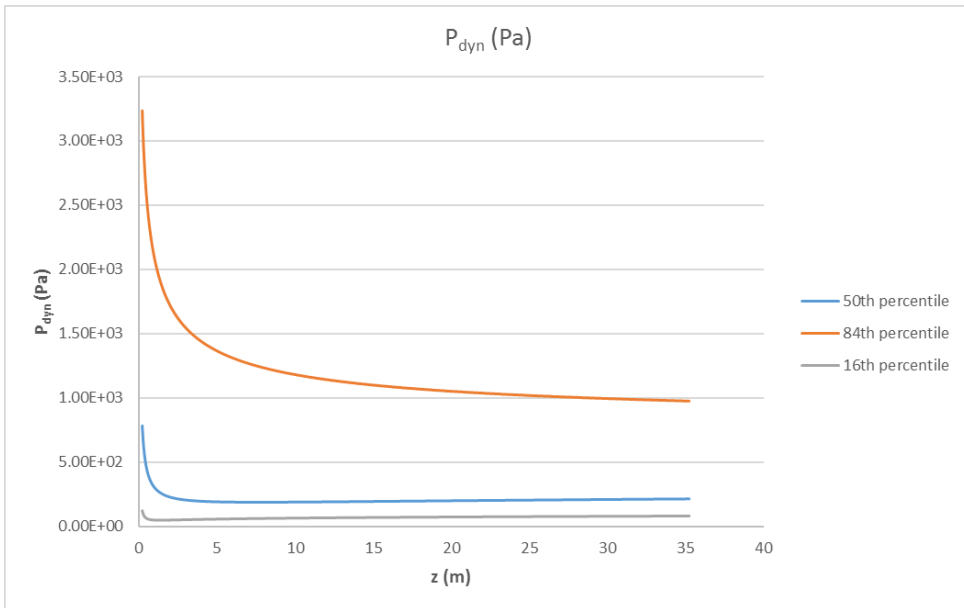


**Fig. 13.** Vertical profiles of dynamic pressure corresponding to the average (blue), maximum (red) and minimum (grey) solution.

## 5. Test cases

---

Two application examples are described in this section. The reader can find the `input.dat` file and results files in the folder “Test cases” included in the PYFLOW package. The test cases are designed to cover the largest possible range of applications and commands; given that a number of possible options are available in the new version of PYFLOW, to show examples with every possible command is out of the scope for this paper. However, it is straightforward to run other cases by simply amending the `input.dat` files of the test cases.

The application examples build on field data collected from laminated pyroclastic flow deposits of Pollena Subplinian eruption (AD 472; Vesuvius, Italy). In particular, we examined deposits of S2 (sample vs 2\_3) and S3 units (sample vs 26\_1) (Sulpizio et al. 2005; 2007), which were emplaced by a dilute pyroclastic current during the second and third phase of the eruption, respectively. Their deposits consist of ash with lenses of lapilli that form low amplitude, meter-spaced dunes with internal cross stratification (Fig. 14).

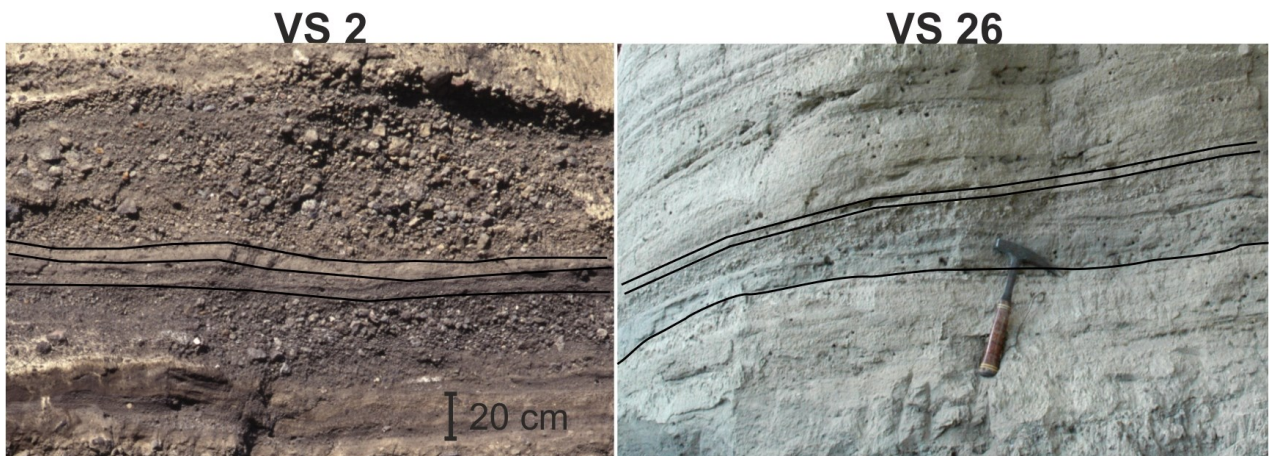


**Fig. 14.** Photos of the outcrops used for the application examples. Left picture: Pollena VS2. Right picture: Pollena VS26. The black solid lines border the portions sampled for the calculations.

In few locations, the deposit show the bedset that reflects the fining upward sequence described in Fig. 1b: a basal layer with inversely graded coarse lapilli, which show an orientation toward flow direction; the laminated layer with cross stratification of fine lapilli/coarse ash and finally the massive fine-ash layer.

### 5.1. Pollena VS2-3

---

In this case we use the “Two layers” method. Fig. 15 shows a screenshot of the `input.dat` file. It is worth noting that any line starting with “!” is ignored by the program and that the order of the entries is not relevant; consequently, the structure of the `input.dat` file shown in Fig. 4 is arbitrary and designed to simplify the reading.

```

! Run control data
MODEL = 'TWOLAYERS'
DEPRATES = .F.
USR_Z_DYNPR = .T.
ZDYNPR(1)=5
ZDYNPR(2)=2
USR_PCX_SOL = .T.
PCX(1) = 0.95
PROBT = 0.05
ZLAMS = 0.001286
! Gas section
MU=2.d-5
DENGAS=0.38

! Deposit section
ZLAM = 0.2
C0 = 0.75
KS = 0.04

! Entrained particle section
DENS_ENT = 2570
DM_ENT = 0.08

! Component 1 section
RHOLAW(1) = 'CUSTOM'
RHOS(1,0)= 1750
D50MM(1) = 1.286
SORTING(1)= 1.54
NCLASS(1)=17
CDLAW(1) = 'DELLINO'
SHAPEFACT(1,0) = 0.47

```

**Fig. 15.** Screenshot of the `input.dat` file of the Pollena VS2-3 application example.

To execute the two layers model, the correct entry is MODEL='TWOLAYERS'. In this case:

- deposition rates are not calculated: DEPRATES=.F.;
- depth-averaged dynamic pressure at two additional heights (5 and 2 m) other than the default 10 m are computed: USR\_Z\_DYNPR=.T., ZDYNPR(1)=5, ZDYNPR(1)=2;
- values of the impact parameters at a probability level of 95% are requested on output: USR\_PCX\_SOL=.T., PCX\_SOL(1)=0.95;
- a significance level of 5% is required for the t-Student test: PROBT=0.05.

From the laminated layer (B in Fig. 1b) we selected the juvenile particles.

In Table 4 input data for the physical variables needed in the calculation are summarized together with the corresponding entries in the input file.

**Table 4.** Input parameters and corresponding commands of the Pollena 2-3 application example.

| <b>Input variable</b>                                     | <b>Value</b>             | <b>Command</b>                       |
|---|--------------------------|--------------------------------------|
| Gas viscosity ( $\eta$ )                                  | $2 \times 10^{-5}$ Pa s  | MU=2.d-5                             |
| Gas density ( $\rho_g$ )                                  | 0.38 kg m <sup>-3</sup>  | DENGAS=0.38                          |
| Layer thickness ( $z_{lam}$ )                             | 0.2 m                    | ZLAM = 0.2                           |
| Concentration at the reference level ( $C_0$ )            | 0.75                     | C0=0.75                              |
| Substrate roughness ( $k_s$ )                             | 0.04 m                   | KS=0.04                              |
| Entrained particle density ( $\rho_{sl}$ )                | 2570 kg m <sup>-3</sup>  | DENS_ENT=2570                        |
| Entrained particle dimension ( $d_l$ )                    | 0.08 m                   | DM_ENT=0.08                          |
| Component 1 density ( $\rho_{s,juv}$ )                    | 1750 kg m <sup>-3</sup>  | RHOLAW(1)='CUSTOM'<br>RHOS(1,0)=1750 |
| Component 1 median grainsize ( $d_{juv}$ )                | 1.286 mm                 | D50MM(1,0)=1.286                     |
| Component 1 sorting ( $\sigma_\phi$ )                     | 1.54                     | SORTING(1)=1.54                      |
| Component 1 number of grainsize classes ( $n_{classes}$ ) | 17                       | NCLASS(1)=17                         |
| Selected drag law for component 1                         | Dellino et al.<br>(2005) | CDLAW(1)='DELLINO'                   |
| Component 1 shape factor ( $\Psi$ )                       | 0.47                     | SHAPEFACT(1,0)=0.47                  |

Results of this test case are summarized in `results.dat`, whose screenshots are shown in figg. 16 and 17.

```

###PROGRAM PYFLOW 2.5 by Fabio Dioguardi###
Data summary
*****TWO LAYER METHOD*****
ENTRAINED PARTICLE
Density of the entrained particle (kg/m^3)      2570.000
Diameter of the entrained particle (m)           0.080

REPRESENTATIVE PARTICLE IN THE OVERLYING LAYER
Particle density (kg/m^3)                      1750.000
Particle equivalent diameter of the median size (mm) 1.286
Sorting particle grainsize distribution (phi)     1.540
Classes number particle grainsize distribution (-) 17
Drag law                                         DELLINO
Shape factor (-)                                0.470

OTHER DATA
Significance level t-test (-)                  0.045
Layer thickness (m)                           0.20000
Particle concentration in the layer (-)       0.001
Substrate roughness (m)                       0.75000
Significance level t-test (-)                  0.040
Layer thickness (m)

Results
50th percentile solution flow density (kg/m^3)      4.509
84th percentile solution flow density (kg/m^3)        2.433
16th percentile solution flow density (kg/m^3)        12.825
50th percentile solution viscous sublayer thickness (m) 0.00129
84th percentile solution viscous sublayer thickness (m) 0.00007
16th percentile solution viscous sublayer thickness (m) 0.00710
50th percentile solution total flow thickness (m)    84.753
84th percentile solution total flow thickness (m)    170.430
16th percentile solution total flow thickness (m)    28.117
50th percentile solution shear flow thickness (m)    7.597
84th percentile solution shear flow thickness (m)    20.369
16th percentile solution shear flow thickness (m)    2.162
50th percentile solution shear velocity (m/s)        2.588
84th percentile solution shear velocity (m/s)        3.525
16th percentile solution shear velocity (m/s)        1.532
50th percentile solution velocity shear stress (Pa) 30.201
84th percentile solution velocity shear stress (Pa) 30.103
16th percentile solution velocity shear stress (Pa) 30.225
50th percentile solution suspension Rouse number (-) 0.840
84th percentile solution suspension Rouse number (-) 0.579
16th percentile solution suspension Rouse number (-) 1.272
50th percentile solution 10m depth-averaged dynamic pressure (Pa) 2896.945
84th percentile solution 10m depth-averaged dynamic pressure (Pa) 6638.296
16th percentile solution 10m depth-averaged dynamic pressure (Pa) 590.109
50th percentile solution 2m particle concentration (-) .15339E-02
84th percentile solution 2m particle concentration (-) .19308E-02
16th percentile solution 2m particle concentration (-) .52462E-03
50th percentile solution 2m depth-averaged particle concentration (-) .67374E-02
84th percentile solution 2m depth-averaged particle concentration (-) .45601E-02
16th percentile solution 2m depth-averaged particle concentration (-) .76230E-02

Test t-Student summary
Significance level      0.022500
Theoretical t value     2.175
Calculated t value     2.174

```

**Fig. 16.** Screenshots of the results.dat file (first part) of the Pollena VS2-3 application example.

```

### User requested outputs ###
z = 5.00
50th percentile solution depth-averaged dynamic pressure (Pa) 3930.566
84th percentile solution depth-averaged dynamic pressure (Pa) 7842.750
16th percentile solution depth-averaged dynamic pressure (Pa) 908.466

###FUNCTIONS VALUES AT USER REQUESTED PERCENTILES###
Percentile = 0.950
Dynamic pressure 10 m
Percentile 0.950
Function value 9744.2952

z = 2.00
50th percentile solution depth-averaged dynamic pressure (Pa) 5890.086
84th percentile solution depth-averaged dynamic pressure (Pa) 9638.561
16th percentile solution depth-averaged dynamic pressure (Pa) 1723.923

Particle concentration 2 m
Percentile 0.950
Function value 0.2121E-02

2 m depth-averaged particle concentration
Percentile 0.950
Function value 0.8029E-02

Flow density
Percentile 0.950
Function value 58.5278

Flow shear velocity
Percentile 0.950
Function value 4.0894

5.00 m average dynamic pressure (Pa)
Percentile 0.950
Function value 10707.8780

2.00 m average dynamic pressure (Pa)
Percentile 0.950
Function value 11944.1965

2 m particle concentration probability function
Symmetrization exponent 2.916
Median 0.62045E-08
Standard deviation 0.59330E-08

2 m depth-averaged particle concentration probability function
Symmetrization exponent 5.021
Median 0.12477E-10
Standard deviation 0.10719E-10

Flow density probability function
Symmetrization exponent -0.650
Median 0.37584E+00
Standard deviation 0.18530E+00

Flow shear velocity probability function
Symmetrization exponent 1.301
Median 0.34458E+01
Standard deviation 0.17038E+01

5.00 m dynamic pressure probability function
Symmetrization exponent 0.731
Median 0.42581E+03
Standard deviation 0.27997E+03

2.00 m dynamic pressure probability function
Symmetrization exponent 1.141
Median 0.19968E+05
Standard deviation 0.15051E+05

```

**Fig. 16.** Screenshots of the results.dat file (first part) of the Pollena VS2-3 application example.

The file is organized as follows: in the first part (“Data summary”), input data for the sedimentological model (Table 4) are summarized for both components; results for the main flow properties (average, maximum and minimum solutions) are subsequently written, followed by a summary of the t-Student test. The file continues with all the user requested outputs, in this case the average specific dynamic pressure at 5 and 2 m height. The following section contains results from the probability density function routine (symmetrization exponent, median  $\mu_{simm}$  and standard deviation  $\sigma_{simm}$ ) for all the considered impact parameters and the values of the impact parameters at the user requested percentile.

Figure 18 shows plots of the vertical profiles of the flow variables as plotted by opening the files concentration\_profile.dat, density\_profile.dat, velocity\_profile.dat, dynamic\_pressure\_profile.dat with Excel.

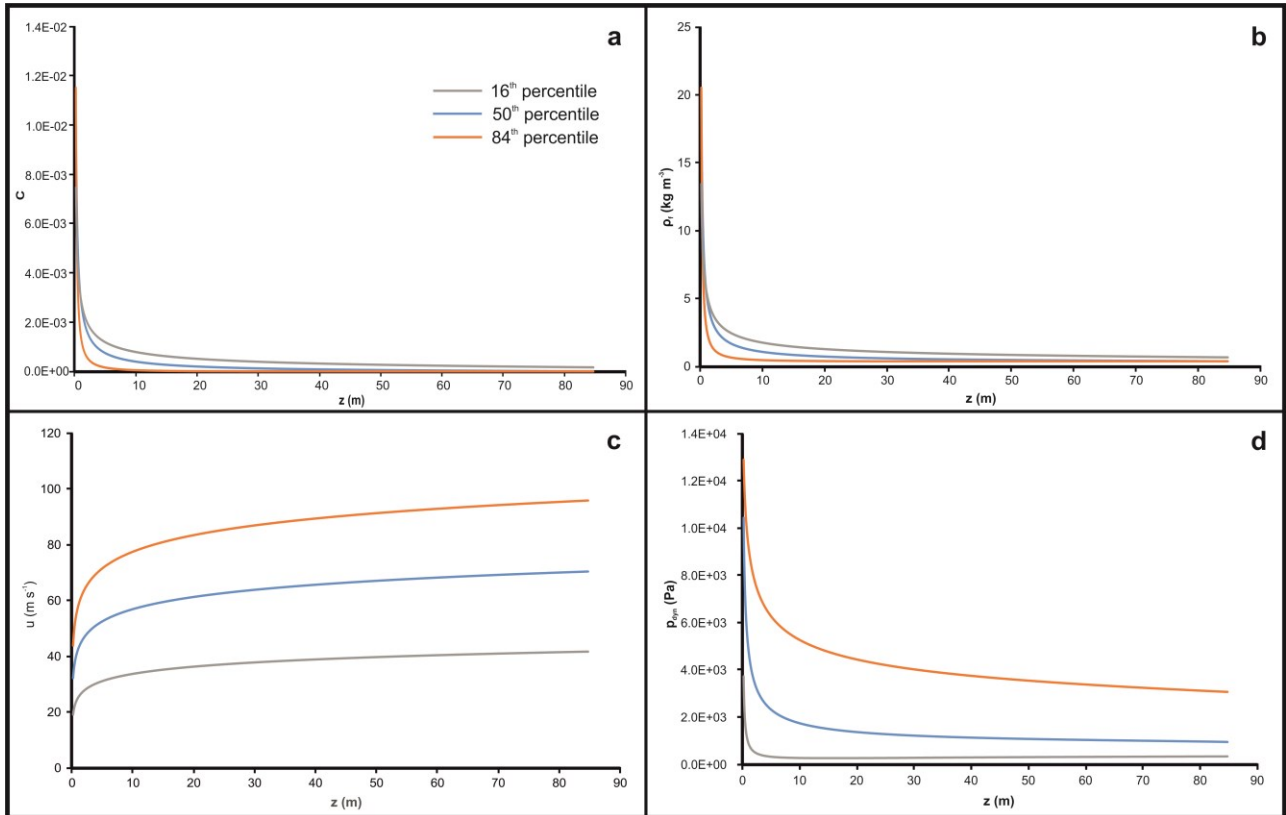


**Fig. 18.** Plots of the vertical profiles of the calculated flow field variables of the Pollena VS2-3 application example. Grey, blue and orange solid lines represent the solutions at 16<sup>th</sup> percentile, 50<sup>th</sup> percentile and 84<sup>th</sup> percentile, respectively. **a.** Particle volumetric concentration  $C$ . **b.** Flow density  $\rho_f$ . **c.** Flow velocity  $u$ . **d.** Flow dynamic pressure  $P_{dyn}$ .

## 5.2. Pollena VS26-1

In this case the “Two components” method was used in conjunction with the depositional model. In fig. 19 a screenshot of part of the `input.dat` file is displayed, as to show the main input data and how to provide the grainsize distribution and the particle density distribution of two of the considered four components.

```

! Run control data
MU=2.d-5
DENGAS=0.38
MODEL = 'TWOCOMPONENTS'
PROBT = 0.05
ZLAM = 0.58
C0 = 0.75
KS = 0.01
DISTRI1 = .T.
DISTRI2 = .T.
DEPRATES = .T.
PN_CUT = .T.
NCOMP = 4
INPUT_WEIGHT='MASS'
DEP_MEDIAN=0.000841468
RHOS_MEDIAN=1881.990269
USR_Z_DYNPR = .T.
ZDYNPR(1) = 2
ZDYNPR(2) = 5
USR_PCX_SOL = .T.
PCX(1) = 0.95

! Component 1 section
RHOLAW(1) = 'POLLENA'
CDLAW(1) = 'DIOGMELE'
SHAPEFACT(1,0) = 0.520
DOTESTCHI(1)=.T.
SIGLEVCHI(1)=0.05
DAVGESPH(1)=0.143
PHIMIN(1)=-2.5
PHIMAX(1)=6.5
DPHI(1)=0.5
WEIGHT(1,1)=15.1
WEIGHT(1,2)=26.6
WEIGHT(1,3)=30.4
WEIGHT(1,4)=27.2
WEIGHT(1,5)=16.5
WEIGHT(1,6)=28.85
WEIGHT(1,7)=30.38
WEIGHT(1,8)=28.35
WEIGHT(1,9)=32.09
WEIGHT(1,10)=26.16
WEIGHT(1,11)=20.37
WEIGHT(1,12)=12.98
WEIGHT(1,13)=14.37
WEIGHT(1,14)=7.58
WEIGHT(1,15)=5.72
WEIGHT(1,16)=3.05
WEIGHT(1,17)=2.13
WEIGHT(1,18)=1.21
WEIGHT(1,19)=0.44

! Component 2 section
RHOLAW(2) = 'CUSTOM'
RHO_CUSTOM(2) = 'CONSTANT'
RHOS(2,0) = 3280
CDLAW(2) = 'DIOGMELE'
SHAPEFACT(2,0) = 0.610
DOTESTCHI(2)=.T.
SIGLEVCHI(2)=0.05
PHIMIN(2)=-1.0
PHIMAX(2)=6.5
DPHI(2)=0.5
WEIGHT(2,1)=0.71
WEIGHT(2,2)=4.78
WEIGHT(2,3)=8.55
WEIGHT(2,4)=9.61
WEIGHT(2,5)=17.64
WEIGHT(2,6)=21.97
WEIGHT(2,7)=22.51
WEIGHT(2,8)=15.62
WEIGHT(2,9)=10.94
WEIGHT(2,10)=12.12
WEIGHT(2,11)=6.39
WEIGHT(2,12)=4.82
WEIGHT(2,13)=2.57
WEIGHT(2,14)=1.79
WEIGHT(2,15)=1.02
WEIGHT(2,16)=0.37

! Component 3 section
RHOLAW(3) = 'CUSTOM'
RHO_CUSTOM(3) = 'CONSTANT'
RHOS(3,0) = 2570
CDLAW(3) = 'DIOGMELE'
SHAPEFACT(3,0) = 0.4
DOTESTCHI(3)=.T.
SIGLEVCHI(3)=0.05
PHIMIN(3)=-3.5
PHIMAX(3)=6.5
DPHI(3)=0.5
WEIGHT(3,1)=9.7
WEIGHT(3,2)=16.2
WEIGHT(3,3)=25.7
WEIGHT(3,4)=32.7
WEIGHT(3,5)=55.0
WEIGHT(3,6)=114.6
WEIGHT(3,7)=119.1
WEIGHT(3,8)=93.05
WEIGHT(3,9)=86.25
WEIGHT(3,10)=74.16
WEIGHT(3,11)=58.08
WEIGHT(3,12)=48.46
WEIGHT(3,13)=33.76

```

**Fig. 19.** Screenshots of part of the `input.dat` file (first part on the left, second part on the right) of the Pollena VS26-1 application example.

In particular, the deposition rates calculation is activated (“`DEPRATES=.T.`”), classes with  $P_n > 5$  are neglected (“`PN_CUT=.T.`”) and the weights for the grainsize analyses are provided in grams (“`INPUT_WEIGHT='MASS'`”). For the juvenile component (component 1) a size-dependent density is selected, in particular the one obtained from this sample (“`RHOLAW(1)='POLLENA'`”) (see Table 5). For each component a Chi-squared test with a significance level of 5% is performed. Table 5 input data relevant for running the two components model are listed.

**Table 5.** Input parameters and corresponding commands of the Pollena 26-1 application examples (only input data for the two components model are shown).

| Input variable  | Value                            | Command                              |
|---|----------------------------------|--------------------------------------|
| Gas viscosity ( $\eta$ )                                  | $2 \times 10^{-5}$ Pa s          | MU=2.d-5                             |
| Gas density ( $\rho_g$ )                                  | 0.38 kg m <sup>-3</sup>          | DENGAS=0.38                          |
| Layer thickness ( $z_{lam}$ )                             | 0.58 m                           | ZLAM = 0.58                          |
| Concentration at the reference level ( $C_0$ )            | 0.75                             | C0=0.75                              |
| Substrate roughness ( $k_s$ )                             | 0.01 m                           | KS=0.01                              |
| Component 1 density ( $\rho_{s,juv}$ )                    | Variable density                 | RHOLAW(1)='Pollena'                  |
| Component 1 median grainsize ( $d_{juv}$ )                | Calculated by grainsize analysis | N/A                                  |
| Component 1 sorting ( $\sigma_\phi$ )                     | Calculated by grainsize analysis | N/A                                  |
| Component 1 number of grainsize classes ( $n_{classes}$ ) | Calculated by grainsize analysis | N/A                                  |
| Selected drag law for component 1                         | Dioguardi and Mele (2015)        | CDLAW(1)='DIOGMELE'                  |
| Component 1 shape factor ( $\Psi$ )                       | 0.52                             | SHAPEFACT(1,0)=0.520                 |
| Component 2 density ( $\rho_{s,xx}$ )                     | 3280 kg m <sup>-3</sup>          | RHOLAW(2)='CUSTOM'<br>RHOS(2,0)=3280 |
| Component 2 median grainsize ( $d_{xx}$ )                 | Calculated by grainsize analysis | N/A                                  |
| Component 2 sorting ( $\sigma_\phi$ )                     | Calculated by grainsize analysis | N/A                                  |
| Component 2 number of grainsize classes ( $n_{classes}$ ) | Calculated by grainsize analysis | N/A                                  |
| Selected drag law for component 2                         | Dioguardi and Mele (2015)        | CDLAW(1)='DIOGMELE'                  |
| Component 2 shape factor ( $\Psi_{xx}$ )                  | 0.61                             | SHAPEFACT(2,0)=0.61                  |

Fig. 20 shows the screenshot of `component1.dat` file, which is written by the grainsize analysis tool.

```

***** GRAINSIZE DISTRIBUTION PARAMETERS CALCULATION FOR COMPONENT 1 *****

Phi    d(mm)    Wt.%    Fr.Cum.Wt    Cum.Wt%
-1.0   2.000    0.50    0.0050    0.5021
-0.5   1.414    3.38    0.0388    3.8823
0.0    1.000    6.05    0.0993    9.9286
0.5    0.707    6.80    0.1672    16.7244
1.0    0.500    12.47   0.2920    29.1988
1.5    0.354    15.54   0.4474    44.7352
2.0    0.250    15.92   0.6065    60.6534
2.5    0.177    11.05   0.7170    71.6993
3.0    0.125    7.74    0.7944    79.4357
3.5    0.088    8.57    0.8801    88.0065
4.0    0.062    4.52    0.9253    92.5253
4.5    0.044    3.41    0.9593    95.9338
5.0    0.031    1.82    0.9775    97.7512
5.5    0.022    1.27    0.9902    99.0170
6.0    0.016    0.72    0.9974    99.7383
6.5    0.011    0.26    1.0000    100.0000

*****CHI SQUARED TEST*****
ztest   Oj      Ej      (Oj-Ej)^2/Ej
-1.19   9.93   11.64   0.25
-0.83   6.80   8.55   0.36
-0.48   12.47  11.50   0.08
-0.12   15.54  13.61   0.27
0.24   15.92  14.20   0.21
0.60   11.05  13.03   0.30
0.96   7.74   10.54   0.75
1.32   8.57   7.51   0.15
5.00   7.93   9.41   0.23

Sensitivity =      0.05
Significance =    0.05
Degrees of freedom = 6.0
Chi calculated =  2.61
Chi tabulated =   12.59

The distribution is not significantly different from a normal standard distribution
COMPONENT 1 GRAINSIZE ANALYSIS RESULTS

phi50 =  1.66435  d50 (mm) =  0.79500
phi84 =  2.36001  d84 (mm) =  0.19479
phi16 = -1.79771  d16 (mm) =  3.47669
sigma =  1.39505

```

**Fig. 20.** Screenshot of component1.dat created by the grainsize analysis in the Pollena 26-1 application example.

In the first part a summary of the grainsize and weight fractions (% and cumulative %) is shown, followed by the section dedicated to the Chi-squared test. Without going in the detail of the output shown in this file (which can be found in the manual), it is to note that the sentence summarizing the results of the test: the distribution is not significantly different from a normal standard distribution. Finally, results from the grainsize analysis are listed, with the grainsize (in phi and mm) at the 16<sup>th</sup>, 50<sup>th</sup> (median) and 84<sup>th</sup> percentile and the standard deviation of the distribution (sorting  $\sigma_\phi$ ). Fig. 21 shows a screenshot of the results.dat file, in particular the part dedicated to the deposition rate and time calculations.

```

###DEPOSITION RATE AND TIME CALCULATIONS
50th percentile solution

*****SUSPENSION LOAD*****
Laminated layer thickness (m) = 0.525E+00
Deposition rate of turbulent suspension (kg m^-2 s^-1) = 0.375E+01
Deposition time of turbulent suspension (s) = 0.264E+03
Total particle concentration of turbulent suspension = 0.538E-02
Total particle concentration of turbulent suspension at deposition = 0.538E-02
Total particle concentration of turbulent suspension remaining at suspension = -0.173E-17

Volumetric sedimentation rate per unit width (m^2 s^-1) = 0.149E-02
Bedload transportation rate per unit width (m^2 s^-1) = 0.521E-02
Srw/Qb ratio (-) = 0.286

84th percentile solution

*****SUSPENSION LOAD*****
Laminated layer thickness (m) = 0.527E+00
Deposition rate of turbulent suspension (kg m^-2 s^-1) = 0.983E-01
Deposition time of turbulent suspension (s) = 0.101E+05
Total particle concentration of turbulent suspension = 0.942E-03
Total particle concentration of turbulent suspension at deposition = 0.942E-03
Total particle concentration of turbulent suspension remaining at suspension = 0.217E-18

Volumetric sedimentation rate per unit width (m^2 s^-1) = 0.390E-04
Bedload transportation rate per unit width (m^2 s^-1) = 0.117E-01
Srw/Qb ratio (-) = 0.003

16th percentile solution

*****SUSPENSION LOAD*****
Laminated layer thickness (m) = 0.525E+00
Deposition rate of turbulent suspension (kg m^-2 s^-1) = 0.847E+01
Deposition time of turbulent suspension (s) = 0.117E+03
Total particle concentration of turbulent suspension = 0.131E-01
Total particle concentration of turbulent suspension at deposition = 0.131E-01
Total particle concentration of turbulent suspension remaining at suspension = 0.000E+00

Volumetric sedimentation rate per unit width (m^2 s^-1) = 0.336E-02
Bedload transportation rate per unit width (m^2 s^-1) = 0.337E-02
Srw/Qb ratio (-) = 1.000

```

**Fig. 21.** Screenshots of the part of the results.dat file of the Pollena VS26-1 application example showing results of the depositional model.

Finally, in fig. 22 the deposition rates of all the grainsize classes for all the 4 components (vesiculated juveniles, pyroxenes, lithic fragments and sialic crystals) are displayed as a function of the grainsize for each solution. Each curve corresponds to a component. These plots were drawn by opening the file deposition\_summary.dat with Microsoft Excel, which includes also the grainsize, terminal velocity, Rouse number, particle density and volumetric concentration for all the components and all the solutions.

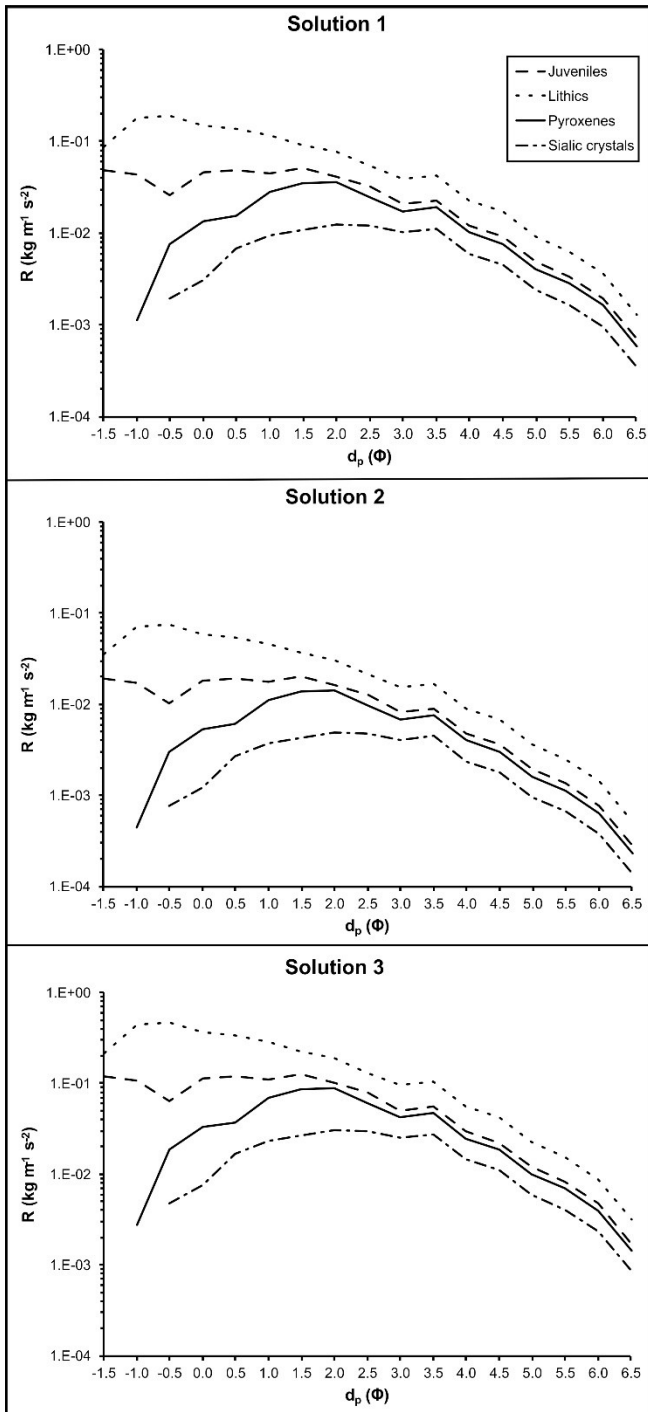


**Fig. 22.** Plots showing the deposition rate vs. particle size for the four components (dashed line: juvenile particles; solid line: pyroxenes; dotted line: lithic fragments; ysolid-dotted line: sialic crystals) of the Pollena 26-1 deposit. Solution 1, 2 and 3 correspond to the average, maximum and minimum solution of PYFLOW, respectively.

## **Reference list**

---

Alfano, F., Bonadonna, C., Delmelle, P., Costantini, L. (2011). Insights on tephra settling velocity from morphological observations. *J. Volcanol. Geotherm. Res.* 208:86–98, doi:10.1016/j.jvolgeores.2011.09.013.

Beckett, F. M., Witham, C.S., Hort, M. C., Stevenson, J. A., Bonadonna, C., Millington S. C. (2015). Sensitivity of dispersion model forecasts of volcanic ash clouds to the physical characteristics of the particles. *J. Geophys. Res. Atmos.* 120:11636–11652, doi:10.1002/2015JD023609.

Branney, M. J., Kokelaar, P. (2002). Pyroclastic Density Currents and the Sedimentation of Ignimbrites. Geological Society, London, Memoirs, 27.

Chien, S. F. (1994). Settling velocity of irregularly shaped particles, *SPE Drill. Complet.* 9:281–288.

Clift, R., Gauvin,W. H. (1971). Motion of entrained particles in gas stream. *Can. J. Chem. Eng.* 49 (4):439–448.

Davies, J. C. (1986). Statistic and Data Analysis in Geology, 2nd ed., John Wiley & Sons, 646 pp.

Dellino, P., La Volpe, L. (2000). Structures and grain size distribution in surge deposits as a tool for modelling the dynamics of dilute pyroclastic density currents at La Fossa di Vulcano (Aeolian Islands, Italy). *J. Volcanol. Geotherm. Res.* 96:57–78.

Dellino, P., Isaia, R., Veneruso, M. (2004). Turbulent boundary layer shear flows as an approximation of base surges at Campi Flegrei (Southern Italy). *J. Volcanol. Geotherm. Res.* 133:211–228.

Dellino, P., Mele, D., Bonasia, R., Braia, G., La Volpe, L., Sulpizio, R. (2005). The analysis of the influence of pumice shape on its terminal velocity. *Geophys. Res. Lett.* 32:L21306. doi:10.1029/2005GL023954.

Dellino, P., Mele, D., Sulpizio, R., La Volpe, L., Braia, G. (2008). A method for the calculation of the impact parameters of dilute pyroclastic density currents based on deposit particle characteristics. *J. Geophys. Res.* 113:B07206. doi:10.1029/2007B005365.

Dellino, P., Büttner, R., Dioguardi, F., Doronzo, D. M., La Volpe, L., Mele, D., Sonder, I., Sulpizio, R., Zimanowski, B. (2010). Experimental evidence links volcanic particle characteristics to pyroclastic flow hazard. *Earth Planet. Sc. Lett.* 295:314–320. doi:10.1016/j.epsl.2010.04.022.

Dellino, P., Dioguardi, F., Doronzo, D. M., Mele, D. (2019a). The rate of sedimentation from turbulent suspension: An experimental model with application to pyroclastic density currents and discussion on the grain-size dependence of flow runout. *Sedimentology* 66(1):129-145.

<https://doi.org/10.1111/sed.12485>

Dellino, P., Dioguardi, F., Doronzo, D. M., Mele, D. (2019b). The Entrainment Rate of Non-Boussinesq Hazardous Geophysical Gas-Particle Flows: An Experimental Model With Application to Pyroclastic Density Currents. *Geophys. Res. Lett.* 46(22):12851-12861.

<https://doi.org/10.1029/2019GL084776>

Dioguardi, F., Dellino, P. (2014). PYFLOW: A computer code for the calculation of the impact parameters of Dilute Pyroclastic Density Currents (DPDC) based on field data. *Comput. Geosci.* 66:200-210, doi:10.1016/j.cageo.2014.01.013.

Dioguardi, F., Mele, D. (2015). A new shape dependent drag correlation formula for non-spherical rough particles. Experiments and results. *Powder Technol.* 277:222-230, doi:10.1016/j.powtec.2015.02.062.

---

Dioguardi, F., Mele, D., Dellino, P., Dürig, T. (2017). The terminal velocity of volcanic particles with shape obtained from 3D X-ray microtomography. *J. Volcanol. Geotherm. Res.* 329:41-53, doi:10.1016/j.jvolgeores.2016.11.013.

Dioguardi, F., Dellino, P., Mele, D. (2018). A New One-Equation Model of Fluid Drag for Irregularly Shaped Particles Valid Over a Wide Range of Reynolds Number. *J. Geophys. Res. Solid Earth* 123(1):144-156, <https://doi.org/10.1002/2017JB014926>.

Dioguardi, F., Mele, D. (2020). PYFLOW\_2.0: A computer program for calculating flow properties and impact parameters of past dilute pyroclastic density currents based on field data. *Bull Volcanol* 80, 28 (2018). <https://doi.org/10.1007/s00445-017-1191-z>

Furbish, D. J. (1997). *Fluid Physics in Geology*. Oxford University Press, New York, 476 pp.

Ganser, G. (1993). A rational approach to drag prediction of spherical and nonspherical particles. *Powder Technol.* 77:143-152.

Haider, A., Levenspiel, O. (1989). Drag coefficient and terminal velocity of spherical and nonspherical particles. *Powder Technol.* 58:63-70, doi:10.1016/0032-5910(89)80008-7.

Hölzer, A., Sommerfeld, M. (2008). New simple correlation formula for the drag coefficient of non spherical particles, *Powder Technol.* 184:361–365, doi:10.1016/j.powtec.2007.08.021.

Houghton, B. F., Wilson C. J. N. (1989). A vesicularity index for pyroclastic deposits. *Bull. Volcanol.* 51:451-462.

Inman, D. L. (1952). Measures for describing the size distribution of sediments. *J. Sed. Res.* 22-3:125-145, doi:10.1306/D42694DB-2B26-11D7-8648000102C1865D.

L'Abbate A. (2007). Calcolo dei parametric fisici di "Correnti pirocastiche di densità" naturali e prodotte in esperimenti. MSc dissertation, University of Bari, Bari, Italy.

Manzaro C. (2005). Ricostruzione delle dinamiche eruttive del vulcano Astroni (Campi Flegrei). MSc Dissertation, University of Bari, Bari, Italy.

Mele, D., Dellino, P., Sulpizio, R., Braia, G. (2011). A systematic investigation on the aerodynamics of ash particles. *J. Volcanol. Geotherm. Res.* 203:1-11. doi:10.1016/j.volgeores.2011.04.004.

Middleton, G. V., Southard, J. B. (1984). Mechanics of Sediment Movement, 2nd ed., Society of Economic Paleonologists and Mineralogists, Tulsa, OK, 401 pp.

Miller, M. C., McCave, I. N., Komar, P. D. (1977). Threshold of sediment motion under unidirectional currents. *Sedimentology* 24:507–527.

Press, W. H., Teukolsky, S. A., Vetterling, W. T., Flannery, B. P. (1996). Numerical Recipes in Fortran 90. The Art of Parallel Scientific Computing. Volume 2 of Fortran Numerical Recipes. Second Edition, Cambridge University Press, 572 pp.

Rouse, H. (1939). An analysis of sediment transportation in the light of fluid turbulence, in Soil Conservation Services Report No. SCS-TP-25, USDA, Washington, D.C.

Schlichting, H., Gersten, K. (2000). Boundary-Layer Theory, Springer, Berlin, 801 pp.

Stow, D.A.V., Bowen, A.J. (1980). A physical model for the transport and sorting of fine-grained sediment by turbidity currents. *Sedimentology* 27:31-46.

Sulpizio, R., Mele, D., Dellino, P., La Volpe, L. (2005). A complex, Subplinian-type eruption from low-viscosity, tephri-phonolitic magma: the Pollena eruption of Somma-Vesuvius (Italy). *Bull. Volcanol.* 67:743-767, doi:10.1007/s00445-005-0414-x.

Sulpizio, R., Mele, D., Dellino, P., La Volpe, L. (2007). Deposits and physical properties of pyroclastic density currents during complex Subplinian eruptions: The AD 472 (Pollena) eruption of Somma-Vesuvius, Italy. *Sedimentology* 54:607-635. doi:10.1111/j.1365-3091.2006.00852.x.

Sulpizio, R., Dellino, P. (2008). Sedimentology, depositional mechanisms and pulsating behavior of pyroclastic density currents, In: Martì, J., Gottsman, J. (Eds.) Calderas Volcanism: Analysis, Modelling and Response, vol. 10, Developments in Volcanology, Elsevier, Amsterdam, pp. 57-96.

Swamee, P. K., Ojha, C. P. (1991). Drag coefficient and fall velocity of nonspherical particles,.J. Hydraul. Eng. 117:660–669, doi:10.1061/(ASCE)0733-9429(1991)117:5(660).

Tran-Cong, S., Gay, M., Michaelides, E.E. (2004). Drag coefficients of irregularly shaped particles, Powder Technol. 139:21–32, doi:10.1016/j.powtec.2003.10.002.

## Symbol notation

---

Latin

| Symbol        | Description   | Units                            |
|---------------|---|----------------------------------|
| $A_r$         | Accretion rate  | $\text{m s}^{-1}$                |
| $B$           | Beta function   | -                                |
| $c$           | Circularity   | -                                |
| $C$           | Particle volumetric concentration   | -                                |
| $C_g$         | Gas volumetric concentration  | -                                |
| $C_d$         | Drag coefficient  | -                                |
| $C_{tot}$     | Total particle volumetric concentration in the flow   | -                                |
| $C_p$         | Specific heat at constant pressure  | $\text{J kg}^{-1} \text{K}^{-1}$ |
| $d$           | Particle dimension  | mm                               |
| $D_{3D}$      | 3D fractal dimension  | -                                |
| $d_{avgeqsp}$ | Diameter of the equivalent sphere of particles selected from the grainsize class were the median lies | phi                              |
| $d_{pr}$      | Equal projected area circle diameter  | mm                               |
| $d_{sph}$     | Volume equivalent sphere diameter   | mm                               |
| $E$           | Expected distribution in the Chi-squared test   | -                                |
| $erf$         | Error function  | -                                |
| $g$           | Gravitational acceleration  | $\text{m s}^{-2}$                |
| $i$           | Index identifying the component   | -                                |
| $j$           | Index identifying the grainsize class   | -                                |
| $k$           | Von Karman's constant   | -                                |

|               |  |                    |
|---------------|--|--------------------|
| $K$           | Degrees of freedom for the Chi-squared test                | -                  |
| $k_s$         | Roughness of the substrate                                 | m                  |
| $m$           | Mass   | kg                 |
| $max$         | Maximum value of the variable for the probability function | Varying            |
| $Md_\phi$     | Median grainsize   | $\phi$             |
| $min$         | Minimum value of the variable for the probability function | Varying            |
| $ms$          | Symmetrization parameter                                   | -                  |
| $m_\phi$      | Slope of the grain-size interpolation function             | -                  |
| $n$           | Degrees of freedom in the t-Student test                   | -                  |
| $N$           | Total number of grainsize classes in the deposit           | -                  |
| $n_{classes}$ | Number of size classes in the grain-size distribution      | -                  |
| $n_{comp}$    | Number of component in the deposit                         | -                  |
| $O$           | Observed distribution in the Chi-squared test              | -                  |
| $p$           | Atmospheric pressure                                       | Pa                 |
| $p_s$         | Particle weight fraction                                   | -                  |
| $P_{dyn}$     | Dynamic pressure   | Pa                 |
| $P_n$         | Average Rouse number                                       | -                  |
| $P_n^*$       | Normalized Rouse number                                    | -                  |
| $q_b$         | Bedload transportation rate                                | $m^3 s^{-1}$       |
| $R$           | Specific gas constant                                      | $J kg^{-1} K^{-1}$ |
| $Re$          | Particle Reynolds number                                   | -                  |
| $Re^*$        | Particle shear Reynolds number                             | -                  |
| $STM$         | Sedimentation Traction Ratio                               | -                  |
| $t$           | t-Student distribution parameter                           | -                  |
| $u$           | Flow velocity  | $m s^{-1}$         |
| $u'$          | Fluctuating velocity in the stream ( $x$ ) direction       | $m s^{-1}$         |
| $u_*$         | Shear velocity   | $m s^{-1}$         |
| $w$           | Particle terminal velocity                                 | $m s^{-1}$         |
| $w'$          | Fluctuating velocity in the vertical ( $z$ ) direction     | $m s^{-1}$         |
| $wt$          | Weight fraction  | %                  |
| $x$           | Stream direction   | m                  |
| $y$           | Variable value in the probability function                 | Varying            |
| $z$           | Vertical direction   | m                  |
| $Z$           | Standard normal distribution                               | -                  |
| $z_{lam}$     | Thickness of the laminated layer in the DPDC deposit       | m                  |
| $z_{sf}$      | Shear flow thickness                                       | m                  |
| $Z_{std}$     | Standardized variable                                      | -                  |
| $Z_{test}$    | Standardized grainsize                                     | phi                |
| $z_{tot}$     | Total flow thickness of the DPDC                           | m                  |

### Greek

| Symbol   | Description            | Units |
|----------|------------------------|-------|
| $\alpha$ | Slope of the substrate | °     |

|                       |  |                    |
|-----------------------|--|--------------------|
| $\alpha_{test}$       | Significance level of the Chi-squared test     | -                  |
| $\beta$               | Corey shape factor                             | -                  |
| $\gamma$              | Flatness ratio                                 | -                  |
| $\Gamma$              | Gamma function                                 | -                  |
| $\Gamma$              | Gamma function                                 | -                  |
| $\eta$                | Gas viscosity                                  | Pa s               |
| $\theta$              | Shield parameter                               | -                  |
| $\mu$                 | Median   | -                  |
| $\rho$                | Density  | kg m <sup>-3</sup> |
| $\sigma$              | Standard deviation                             | -                  |
| $\sigma_\phi$         | Sorting  | $\phi$             |
| $\tau$                | Shear stress                                   | Pa                 |
| $\tau_0$              | Shear stress at the base of the current        | Pa                 |
| $\varphi$             | Sphericity                                     | -                  |
| $\varphi_{\parallel}$ | Longwise sphericity                            | -                  |
| $\varphi_{\perp}$     | Crosswise sphericity                           | -                  |
| $\phi_{16}$           | 16th percentile of the grain-size distribution | $\phi$             |
| $\phi_{3D}$           | 3D Sphericity                                  | -                  |
| $\phi_{50}$           | 50th percentile of the grain-size distribution | $\phi$             |
| $\phi_{84}$           | 84th percentile of the grain-size distribution | $\phi$             |
| $\chi$                | Chi distribution                               | -                  |
| $\psi$                | Particle shape factor                          | -                  |

## Subscripts

| Symbol    | Description                        |
|-----------|------------------------------------|
| $0$       | Reference level in the DPDC        |
| $I$       | Entrained particle                 |
| $atm$     | Atmosphere                         |
| $avg$     | Average value                      |
| $dep$     | Deposit                            |
| $f$       | Fluid phase                        |
| $g$       | Gas                                |
| $juv$     | Juvenile component                 |
| $m$       | Magmatic component                 |
| $massive$ | Massive layer                      |
| $mod$     | Model value                        |
| $norm$    | Value normalized to real data      |
| $s$       | Solid phase (particles)            |
| $simm$    | Simmetryzed parameters             |
| $sp$      | Value specific to a certain height |
| $sph$     | Equivalent sphere                  |
| $sphere$  | Spherical particle                 |
| $susp$    | Turbulent suspension               |

|             |           |
|-------------|-----------|
| <i>tot</i>  | Total     |
| <i>wash</i> | Wash load |
| <i>xx</i>   | Crystals  |